AN ABSTRACT OF THE THESIS OF

Vardan M Rathi for the degree of Master of Science in Material Science and Wood Science presented on March 20, 2009

Title: Bending Property Enhancement of Wood Strand Composite using Viscoelastic Thermal Compression.

Abstract approved:

Frederick A. Kamke Rakesh Gupta

The fundamental intent of the study was to develop an innovative wood-strand composite for use in structural applications. Plantation grown, low density, hybrid poplar was used in the study which was found to be appropriate for the underlying Viscoelastic Thermal Compression (VTC) process. Wood modified by this process has high density and a proportional increase in its flexural strength and stiffness. The VTC process increases the density of wood in the presence of steam, which acts as a plasticizer, mechanical compression and high temperature. Steam pressure is manipulated to induce the mechanosorptive effect during VTC processing, increasing density without fracturing the cell walls. There were three components of this research project. Firstly, the scale-up VTC device was successfully constructed to process samples of dimension: 61 x 25 cm (24” x 10”). Secondly, the influence of high density VTC wood strands in an oriented strand

composite was evaluated. The novelty of this objective was that the overall panel density was not increased. Lastly, a three-layer laminated composite was made, where the lamina were comprised of wood strand panels that were VTC processed prior to lamination.

Both methods of VTC composite manufacture improved bending properties in comparison to control specimens. Two treatments were studied for the VTC strand composites. The treatments included the addition of 20% and 40% of VTC strands, by weight, oriented on the surface of the panel. Panels with 20% by weight of VTC strands oriented on the surface showed no statistically significant increase of MOE and MOR. The addition of 40% VTC strands improved the MOE and MOR by 30% and 18%, respectively. The MOE of the strand composites that were processed by VTC increased by approximately 150% to 160%. The VTC laminates were then bonded to produce the final three-layer product. Visual inspection revealed that the VTC process did not disrupt the phenol-formaldehyde bond.

Bending Property Enhancement of Wood Strand Composite using Viscoelastic Thermal Compression.

by
Vardan M Rathi

A THESIS

submitted to

Oregon State University

in partial fulfillment of
the requirements for the
degree of

Master of Science

Presented March 20, 2009
Commencement June 2009

Master of Science thesis of Vardan M Rathi presented on March 20, 2009

APPROVED:

Co-Major Professor, representing Material Science

Co-Major Professor, representing Wood Science

Director of the Material Science Program

Head of the Department of Wood Science and Engineering

Dean of the Graduate School

I understand that my thesis will become part of the permanent collection of Oregon State University libraries. My signature below authorizes release of my thesis to any reader upon request.

Vardan M Rathi, Author

TABLE OF CONTENTS

Page

TABLE OF CONTENTS (Continued)

Page

LIST OF FIGURES

Figure Page

LIST OF FIGURES (Continued)

Figure Page

LIST OF FIGURES (Continued)

Figure Page

LIST OF TABLES

Table Page

Chapter 1: Introduction

Mental abstraction put to physical realities is the root of scientific research and development. The Tao, whether it be the rule, law or the way, of human thought is mostly to material things; and if one begins with psychology, it is not as a metaphysician who loves to lose himself in heavenly uncertainty, but as a realist to whom thought, however distinct it may be from matter, is essentially a mirror of external and physical reality. It's the thought that defines the idea and humans give this idea desired shape. This research focuses on one such thought.

Global wood use is on the rise. Increase in population in conjunction with per capita income growth will strongly influence the demand for wood (Clark, 2001). The recent exponential demand has been constrained by a diminishing, or more restricted, forest supply base, unwillingness to make long-term financial commitments, and high conservation demands. Hence, grown forest plantations, forest thinnings, and smaller diameter trees are focused upon to supplement wood resources. But the issue of concern with wood grown from the above sources is the lack of desirable material properties. Density and mechanical strength are worst affected and hence cannot be utilized for structural applications, where stiffness and strength is a requisite. Enhancement of the low quality wood, therefore, would be paramount in ensuring business profitability. This would require intensified treatment in the innate stages of the processing to yield the desired product. Economic sustainability of the product is also the key by which it survives the ever growing industrial competition. Viscoelastic Thermal Compression (VTC) of wood is one such treatment which greatly improves material properties (Kamke 2000). It involves the thermal compression of wood

perpendicular to the grain in the presence of steam, which acts as plasticizer and results in densification without fracturing the cell wall. Partial hydrolysis of the hemicelluloses and auto reaction also occur due to the presence of steam, which in turn increases stiffness in a greater proportion relative to the density. The innovation in this process is the utilization of the mechanosorptive nature of the wood by manipulated release of moisture during compression. VTC wood is not proposed to be used independently as it poses some challenges with dimensional stability; rather it can be employed as a component in a composite lay up.

Oriented wood strand composites are designed to meet the needs of a particular objective. In the building construction industry, these composites find varied applications such as sheathing material for walls, roofs, and floors. However, to efficiently engineer wood composite products, it is important to understand the material and manufacturing variables affecting their elastic and strength behavior. With oriented strand composites (OSC) replacing sawn lumber and plywood for many structural applications, such as girders, beams, headers, joists and columns, accurate representation of their material properties is mandatory. The intrinsic properties of the virgin wood from which the strands are created impart certain limitation on the resulting composite properties. The positive feature of manufacturing composite panels lies in the engineering and manipulation of the directional properties to the advantage of their application.

This research lays its emphasis in putting forth a technology to develop highly engineered wood strand composites using wood modified by the VTC process. The specific objectives of this research are threefold:

1. Construct a VTC device to process oriented strand composites.
2. Evaluate the influence of VTC wood strands on the mechanical properties of an oriented strand composite.
3. Evaluate the mechanical properties of an oriented strand composite that has been modified by the VTC process.

Chapter 2: Literature Review

2.1 Background

Insufficient mechanical properties of wood can be modified by varying successions of thermal, mechanical compression and steam treatments. Density is the prime indicator of the mechanical properties of wood (Hoadley 2000). Wood can be densified by various means; one involves a chemical impregnation of its void volume with polymers, molten metals, natural resins, waxes etc. Compression of the wood cells in the transverse direction can also be obtained under conditions that do not cause damage to the cell wall (Kollmann et al. 1975). Wood when compressed perpendicular to the grain behaves like a cellular material (Wolcott et al, 1989; Li et al, 1990). However, wood compressed perpendicular to the grain beyond the yield strength, results in cell collapse (Navi and Girardet 2000). The primary goal behind the compression or densification of wood is the reduction of the available void spaces in the total wood volume (Tomme et al. 1998). Low to medium density wood is usually the most suitable raw material for wood densification due to inefficient material properties and mechanical strength (USDA 1999).

Two methods of densification developed at the U.S. Forest Products Laboratory are Compreg (Stamm and Seborg 1941) and Staypak (Seborg et al. 1962a). Compreg is comprised of veneers infused with phenolic resin, which then dries and congregates under heat and pressure. The moisture resistance and compressive strengths of the product was

amplified by the resin treatment. However, the composite was more brittle as indicated by reduced tensile, toughness, and impact values. In contrast, Staypak is produced by compressing wood with high heat stability and controlled moisture content, without any resin. To eliminate spring back, wood should be pressed under conditions that cause sufficient flow of lignin. The extreme compression and thermal degradation products apparently promoted natural crosslinking between the polymers in the cell wall. This resulted in wood possessing improved strength and stiffness with about twice the toughness and impact strength of Compreg. However, dimensional stability of the wood was an area of concern due to the absence of resin (Erickson 1965).

Wood composites in the present era are identified with such names as oriented strand composites (OSC), plywood, glulam, laminated veneer lumber (LVL) etc. OSC is the focal point of the current review. OSC are of two types: Oriented strand board (OSB) and laminated strand lumber (LSL). Oriented strand board is essentially a structural panel made from thin wooden strands that are sprayed with resin, formed into three distinct layers, and compressed at elevated temperatures to cure the resin and obtain the necessary bonding. The adjacent strand layers are oriented, with respect to the long axis of the strand, perpendicular to each other. The wood strands used are normally obtained from low to medium density species such as aspen, yellow-poplar, southern yellow pine, red maple, sweetgum etc. Wood strands with an aspect ratio of at least 3, when oriented to produce a panel, provide a product with improved bending strength and stiffness in the aligned direction (FPL-GTR-149, 2003). OSB being an engineered product, has the primary advantage of being custom

made to meet the specific requirements of thickness, density, strength, rigidity, panel size and surface texture (Structural Board Association, 2000). It is extensively used as components for I-beams, roofs, floor sheathing, trusses, stressed skin panels, sandwich panels and structural insulated panels. It also finds application in crating, bins, furniture, frames, display racks, decorative paneling etc.

Alternatively, LSL is a composite material which is comprised of unidirectional oriented wood strands, roughly 300 mm long, which are sprayed with resin and compressed to form billets that are about 90 mm thick. It is usually produced from smaller diameter and lower quality trees. The material and mechanical properties of the LSL are dependent upon the wood species, density and orientation. To a significant degree, the strength and stiffness are directly related to the species and density in both the composite and the wood. Strand orientation is a limiting factor in the manufacturing process. It has been shown that orientation improved the axial and bending stiffness as well as the strength properties in specific loading applications (Hunt and Suddarth 1974; Hoover et al. 1992). LSL generally finds its application in structural building elements such as beams and columns. Also, LSL is differentiated from OSB by its longer strands and greater board thickness.

Sandwich composites, are increasingly being used in structures where the predominant loads are flexural, with strong and stiff facings and lightweight cores. In these structures, the thin facings resist nearly all the in-plane load and bending moments. The core layer usually imparts the shear rigidity. The primary goal of the sandwich structure was to provide

material with a high stiffness to weight ratio. The effective MOE of the sandwich is dependent upon the MOE of each layer (Bodig and Jayne 1982). Board MOE can then be determined based on the mechanics of composite materials by considering all the moduli of the layers (Suo and Bowyer, 1995).

2.2 Dimensional stability

Wood is highly anisotropic with regard to dimensional stability in response to moisture content changes. The change in dimensions is least in the longitudinal direction, greater in the radial direction and maximum in the tangential direction (Hoadley 2000). Hygroscopicity, in combination with the density and structure of wood, is the primary reason for the magnitude of shrinkage and swelling. Dimensional instability of wood has been both a bane and a boon, but the adverse effects have initiated efforts to mitigate this property. Extensive studies have been conducted pertaining to dimensional stabilization of wood by numerous methods (Stamm and Hansen 1937; Hillis 1984; Hsu et. al. 1988; Kawai et al. 1992; Inoue et al. 1993 and Inoue et al. 1996). These included mechanical modification, water repellent coating, bulking treatment, and reduction of hygroscopicity as summarized by Rowell et al. (1981). Hence, for densified wood it is important to properly define the pressing conditions under which the spring-back or recovery from compression is minimized.

Wood-based materials seek consideration due to the fact that their dimensions change by greater amplitude with changes in relative humidity compared to dimensional changes stimulated by temperature effects (Bryane 1962). Comprehensive studies have been done on perpetual strength loss, sometimes leading to failure because of thickness swelling or out of plane swelling (Hsu 1987; Liu and McNatt 1991; Wu and Suchsland 1997). Furthermore, wood composites often demonstrate a high degree of dimensional instability compared to solid wood. The rate of shrinkage or swelling is directly proportional to the amount of water being adsorbed or desorbed from the wood or it's composite (Rowell, 2005). Hence higher density will yield a higher rate of water transport and thus more potential for shrinkage or swelling. Another factor contributing to the impermanence of the dimensions could be the release of built up stresses in the wood that develop during the tree growth, storage or manufacturing process. This results in a breaking of the adhesive bond and internal crosslinking which leaves the wood in a completely tumescent state (Hsu et al. 1988).

2.3 Influence of heat and steam treatment

Wood strength decreases linearly as the temperature is increased in a given range (Kollman and Cote 1968, Gerhards 1982). The immediate effect of heating wood is dehydration. Sometimes upon exposure to higher temperatures, an increase in the plasticity of the lignin is noticed along with an increase in spatial size, hence, reducing the intermolecular contact. Such changes in wood are usually recoverable. But, when wood is subjected to high temperatures for prolonged periods of time, the cellulose and the hemicelluloses slowly start

to depolymerize which gradually leads to pyrolysis and volatilization of cell wall polymers (LeVan et al. 1990).

Sequences of studies on the heat stabilization of wood were started by Stamm and others at the U.S. Forest Products Laboratory in the early 1930's. It was shown that high temperature treatment of wood reduced its hygroscopicity, and while making it more dimensionally stable, a marked drop in the strength of the product was observed. In this process wood loses xylose, galactose, and arabinose. Loss of arabinose was reported to be the most significant and is believed to be responsible for the initial strength loss. It was therefore inferred that high temperature alone can deteriorate the cellular structure.

Noticeable drops in the modulus of rupture (MOR), modulus of elasticity (MOE) and compression strength were noticed when wood was treated at about 200°C in the presence of moisture (Giebeler 1983). These permanent thermal effects on strength are indicative of changes in the polymeric substance and structure of the wood. Hillis (1984) also reviewed the effects of high temperature and chemicals on wood stability. Gerhards (1982) claimed that the strength of wood is reflective of the temperature of the working environment, albeit at a constant moisture content. Compression of moist wood at high temperatures produced a stabilized product (Seborg et al. 1962a). Though wood, when treated in wet conditions at high temperature degrades ten times faster when compared to the dry wood (Skaar 1976)

Wood, a hygroscopic material, depletes or replenishes water in the fiber cell wall so as to be in equilibrium with the relative humidity of the immediate ambient environment. This results in an inconsistency in the wood material and variability in the mechanical properties (Wilson 1932, Gerhards 1982). Water in wood exists in three basic forms: bound water which is accumulated in the hygroscopic cell wall, free or capillary water which resides in the voids within the wood, and water vapor that also resides in the voids. Fiber saturation point (FSP), as defined by Tiemann (1906), is the moisture content where the cell walls reach saturation while the cell cavity is free of liquid water. Moisture content, when varied between oven dry (OD) and FSP, affects the strength and reduces the hydrogen bonding between the organic polymers within the cell wall, and hence, furthering its aftermaths to the other material properties as well (Rowell 1980).

Several researchers have studied the effect of heat and pressurized steam on wood (Kamke and Casey 1988b; Kawai et al. 1992; Inoue et al. 1993 & 1996; Dwianto et al. 1998; Rowell et al. 2002; Heger et al. 2004). The viscoelastic and thermal properties of the amorphous content of wood was found to be sensitive to heat and steam, which acts as a plasticizer, whereas the properties of semi crystalline cellulose are mainly dependent upon the degree of crystallinity (Salmen and Black 1977). It was noticed that wood, when subjected to steam, softened or initiated the flow of polymers in the cell wall and reduced the compression force required for densifying the composite. Hsu and his coworkers (1988) proposed that steam pretreatment greatly reduces springback. Partial hydrolysis of the hemicellulose was claimed to be the reason for dimensional stability. It was later found that the

polysaccharides that were released due to the hydrolysis of hemicellulose in the presence of steam reached a maximum and then started to decrease with prolonged steaming (Lawther et al. 1996). Hence, the inference drawn from the research was that free sugars that were released re-reacted to form various other products which were found to be beneficial. Post-compression steaming resulted in complete fixation and the realization that the extent of restoration to original state was minimized with increased temperature and extended press time. Improved mechanical properties were obtained when steam injection pressed (Kawai et al. 1992).

2.4 Viscoelastic behavior of amorphous polymers in wood

Elastic theory is based on the regaining capacity of the material to its original dimensions when it is released from a given stress. The inverse behavior is viscosity, or even termed as plasticity, where the material stays in the compressed or the deformed state even after the stress applied is removed. Wood is considered a viscoelastic material. The creep phenomenon is explicated by the viscoelastic behavior in which a given load actuates an instantaneous deformation, and persistence of the constant load would lead to supplementary secondary permanent deformation.

It is well known that the major constituents of wood are cellulose (mainly crystalline), hemicellulose and lignin (amorphous polymers). The glass transition temperature (T_g) is the temperature at which the amorphous polymer changes from a hard glassy form into a rubber

like plastic or viscous form. This is contingent upon the temperature, time and diluent concentration (Back and Salmen 1982; Wolcott et al. 1990). The transition from the glass to the rubbery state in polymers is observed by monitoring rapid changes in mechanical or physical properties such as elastic modulus, specific volume, heat capacity and dielectric behavior with increasing temperature. Viscoelastic polymers, hemicelluloses, lignin and amorphous cellulose exhibit individual glass transition temperatures. Cellulose softens at 200-230 ºC, depending on the crystallinity index. But in the presence of water, the T_g is moderated. As shown by Salmen and Back (1977), cellulose is plasticized by water and its T_g recorded a 20 ºC drop at 30% MC. The energy essential to instigate chain mobility is also decreased due to plasticization of the cellulosic compounds (Kelley et al 1987). Hemicelluloses soften at a lower temperature range of 165-175 ºC and dry lignin softens in the proximity of 200 ºC (Irvine 1984; Goring 1963). Water saturated hemicellulose displays sub-ambient T_g, similar to cellulose. Essential properties of the wood are moderated when the individual amorphous polymers surpass their respective softening point.

When amorphous polymers in the wood are heated beyond their T_g, stiffness drops considerably. This decline is characterized by the available thermal energy being adequate enough to overcome the rotational energy barriers in the chain and the reduction of the activation energy (Cowie 1991; Kelly et al.1987). When heated beyond 160 °C, lignin begins to flow and reduces the permeability of wood which in turn restricts the adsorption of moisture (Chawla and Sharma 1972). Hemicelluloses are highly unstable to thermal effects and degrade faster than the cellulose (Stamm 1964). However, the magnitude of degradation

was time, temperature and moisture content dependent. Lignin on the other hand is less hydrophilic thereby limiting water's impact on the material property, helping in the retention of the strength and stiffness. A previously conducted study indicated that the consequence of heating wood under steam pressure, increased cellulose crystallinity (Inoue et al. 1993). Gardner et al. (1993) furthered their views, stating that the rise in cellulose crystallinity also indicated an increase in the elastic modulus. It was also observed that the flake strength and stiffness increased with increasing temperature. Cell walls show viscoelastic behavior when wood is compressed in the direction perpendicular to the grain (Wolcott et al, 1990 and 1994; Lenth and Kamke, 2001b). Kawai et al. (1992) examined the properties of the steam pressed laminated veneer lumber (LVL). He observed reduced spring-back at high steam pressure but at the same time obtained lower MOE values. The rationale suggested was the degradation of the cellulose microfibrils.

Wood is an intricate polymer composite with diverse molecular domains. Prominent transition of the behavior of the isolated individual wood polymers has been noted in situ (Hillis and Rozsa 1978; Kelley et al. 1987). There are both static and dynamic analytical methods available to estimate and interpret the glass transition of amorphous polymers. These include static methods, such as differential scanning calorimetry (DSC), differential thermal analysis (DTA) and thermo gravimetric analysis (TGA), and dynamic methods such as dynamic mechanical analysis (DMA), dielectric thermal analysis (DETA) and torsional pendulum analysis. More than one transition has been observed using the above mentioned dynamic analytical methods.

2.5 Hot-Pressing variables and its influence on the OSB

OSB is manufactured by pressing an accumulated mass of adhesive blended flakes to a given thickness. There are three methods available for hot-pressing the mat: conventional uni-axial platen press, continuous belt press, and a steam-injection press. The uni-axial platen press is a traditional method of hot-pressing and is a batch operation. This process involves either two platens parallel to each other or multiples of such platens stacked together. The platen setup is attached with hydraulics and heating elements that provide the required compression force for densification at elevated temperature. A belt-press is usually employed in the industry for continuous mass production of OSB sheets. The device consists of two calibrated roller-rod belts running between a solid steel belt and hot platens. Pressure is applied using hydraulic cylinders that are mounted in numerous press frames positioned along the length of the press. Consolidation pressure is independently controlled across the width and length of the press. The recent and more advanced method of hot-pressing is the steam injection press (SIP). This press is similar to the uni-axial hot-press, but contains small holes on both the platens for the inlet of the steam into the mat while manufacturing OSB. Steam injection along with mat consolidation rapidly transfers heat throughout the wood particulate mat resulting in a faster cure of the thermosetting resin. Geimer and Kwon (1999), observed that SIP mats showed an improved thickness swell which was proportional to the steam time and pressure. However, bending properties of the SIP mats were lower compared to that of conventional OSB. Hot-pressing of the mats to a restricted degree is a passive, inefficient and uncontrolled VTC process.

The bending and compression strength of the final panel are dependent on numerous factors: the moisture content of the flakes and mat, density of the strands (face/core), uniform blending, mat forming/orientation, pressing temperature and time, pressing environment, type of resin and its content in the panel. Even small variations in these parameters might dramatically change the strength and stiffness of the OSB.

Higher resin solids content in the mat greatly enhances mechanical properties such as the MOE, MOR and internal bond (IB) strength (Wilson, 1982; Sun et al. 1994a). However, it also makes the composite more brittle and susceptible to thickness swell and linear expansion (Wilson, 1982; Sun et. al., 1994b). Semple et al. (2007) reported that fast grown and larger diameter wood having low initial density from hybrid poplar is highly suitable for the production of OSB. Panels made out of low density wood had improved properties such as mat compaction and bond strength. However, bending properties were not influenced by the density adjustments.

During hot-pressing, moisture movement resulted in considerable density changes as measured by the in-press radiation-based system (Winistorfer et al. 2000). Wu and Suchsland (1997) studied that OSB's manufactured from aspen and southern pine illustrated linear decline in MOE and MOR with increasing moisture content. An increase in moisture content also showed proportional but non-linear variations in linear expansion and thermal swell of the composite board (Wu and Piao, 1999). It was also indicated that initial mat

moisture content influenced the transport phenomena of differential heat and mass and made them interdependent. The latent heat of vaporization of water appreciably leaves its impression on the temperature rise in the mat during hot-pressing.

The spatial structure of a wood composite panel impacts the dimensional stability, density distribution, mechanical/material properties, and compaction behavior of the final product. The mechanical forces imposed on the strands, and the corresponding response, is decided by the placement of the strands in the OSB mat (Price, 1976; Geimer et al., 1985; Casey, 1987). Strands in the face region are subjected to different hygro-thermal treatment than those from the core region during hot-pressing (Kamke and Casey, 1988b). To achieve a necessary transfer of applied stress within the mat, the flakes have to be long enough to allow adequate overlap (Laufenberg 1984, Barnes 2001). When long flakes are used in the manufacturing of oriented strand composites, the waviness along the length of the strand through the thickness of the composite could also moderate its mechanical properties. In addition, the degree of orientation of the strands affects the strength and stiffness of the wood composite. Garcia et al. (2003) showed that the flake alignment affects the horizontal temperature and pressure gradient in the oriented direction and hence, affects the density distributions.

Wood, when compressed under extreme heat, pressure and varying environmental conditions for different durations, may change its mechanical properties and such disparities may impact the final product. The nonlinear mechanical properties of wood strands, when

compressed in the transverse direction, were explained using the elementary theories of cellular material and viscoelasticity of polymers (Wolcott et al, 1994). As the mat is hot-pressed, the particles deform during bending and compression, and thus undergo plastic deformation. Temperature and moisture gradients cause weakening of particles and the overall effect results in a vertical density profile. The strand densification is mainly influenced by the spatial structure, degree of contact between the particles, and the temperature and moisture gradients (Steiner and Dai 1993; Laufenberg 1984; Kamke and Casey 1988a).

Press closing time is a crucial parameter in the hot-pressing schedule and aids in controlling the density distribution. Extended closing time results in more stress relaxation before achieving the final thickness. This in turn affects the pressure and temperature distributions in the mat. Miyamoto et al (2002) reported that increased press closing time corresponded, to some extent, to an increase in the core density. There was also a shift of the peak density noticed from the face layer to the core layer and resulted in lower MOE and MOR. The lower MOR was attributed to the low density and a procured layer in the surface regions of the board.

Chapter 3: Materials and Methods

The hybrid poplar to be used in this project is a clone of *Populus deltoides* and *Populus trichocarpa*. It was grown on a plantation in Clatsop County, Oregon and harvested in 2007. The trees were 18 years old and had a diameter of 30 – 36 cm. The clone is a low-density species with an oven-dry density of approximately 0.35 g/cm^3. The obtained logs were sawn into 25 mm (1-inch) thick boards and then cut into 152 mm (6 inch) strands using a vertical knife slicer so the compression to be obtained is perpendicular to the grain. Strands of two different thicknesses were manufactured. Strands of dimension 140 x 25 x 2.3 mm were used to manufacture VTC strands. On the other hand strands of dimension 152 x 25 x 0.6 mm (6 x 1 x .025 inch) were the normal strands used in the strand composites manufacturing.

3.1 Construction of the VTC device

The modified VTC device is an engineered scale-up device which can make samples that are 61-cm (24-inch) in length and 25.4-cm (10-inch) wide. It follows the same fundamental operation of the smaller scale VTC device (O'Conner 2007), but has a different mechanism of compression and steam production. The modified device is a stainless steel reaction chamber of variable volume. This flexible volume is achieved with a 71-cm (28-inch) diameter, stainless steel bellows. It utilizes an already available 91-cm by 91-cm (36-inch by 36-inch) hot-press. The hot-press has a hydraulic power unit which can supply up to 4450

KN (1,000,000 pounds of force). The platens of the press are independently heated. The lid of the device, which grabs most of the attention, is attached to the bellows using 14 bolts. The compression force from the hot-press and a gasket between the lid and the container provide the necessary sealing of the pressure. The platens, where the sample is placed, are attached to the bottom surface of the lid. Using a ceramic insulation, the platens are thermally isolated from the lid. The platens are also accoutered with external heating elements so as to provide independent control of temperature. The lid is made up of a layer of stainless steel and easily available machine steel. Stainless steel is used for the surface which is exposed to the pressurized steam inside the vessel. The rest of the lid is comprised of machine steel which allows cooling water inlet and outlet, electrical cables, thermocouples, water for steam production and steam exit. With the known minimum volume of the chamber, the amount of water required to pressurize the vessel with saturated steam at 861 kPa (125 psi) and 175 ºC was calculated. Prior to processing the samples, the device was preheated using the hot-press platens.

3.2 Oriented strand composite (VTC strands):

The VTC device was used to produce the VTC strands. The VTC device, as shown in Figure 3.2.1, is a 50 liter stainless steel chamber designed to hold a saturated steam pressure of 0.8MPa (125 psi) at 175 ºC. The setup includes an ENERPAC hydraulic ram, which can apply pressure in the range of 0 - 8.3 MPa (0-1200 psi), surmounted on the lid. The lid also accommodates an entry and exit valve for the steam to pressurize the vessel. The above

mentioned steam is obtained from a boiler which can supply up to 1 MPa (150 psi) of steam pressure. This lid attaches to the chamber with 6 (out of the 12 available holes in the lid), ¾-inch, evenly spaced bolts with a gasket in between. The target temperature is obtained through two heating jackets that surround the stainless steel cylinder, which is approximately 152-cm (5 feet) in height and 25.4-cm (10-inch) inside diameter. There are six steel plates, four in the middle and one each on top and bottom, (approximate dimensions: 140 x 140 x 25.4-mm (5.5 x 5.5 x 1-inch)) that are stacked using four rods on the corner of each plate (Figure 3.2.2). These rods are attached to the bottom of the lid. The hydraulic force from the ram is transferred to these plates via a movable cylinder that is located inside the bellows, which provides free vertical motion and, at the same time, keeps the pressure in the vessel intact. The samples, along with the spacers, were placed in between these steel plates and in one batch, 18 samples (strands) were processed. The thickness of the VTC strand was controlled by the thickness of the spacers placed between the steel plates.

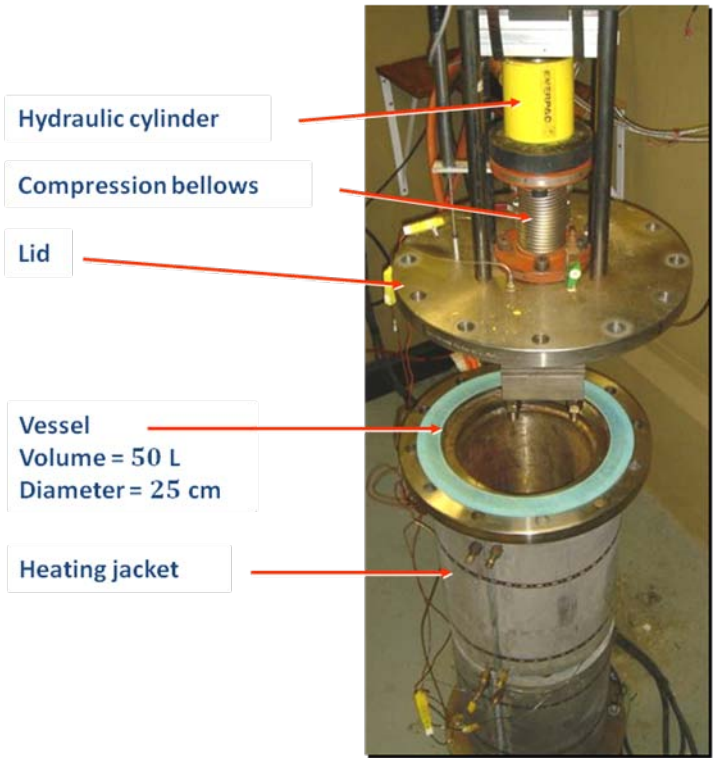

Figure 3.2.1: VTC device.

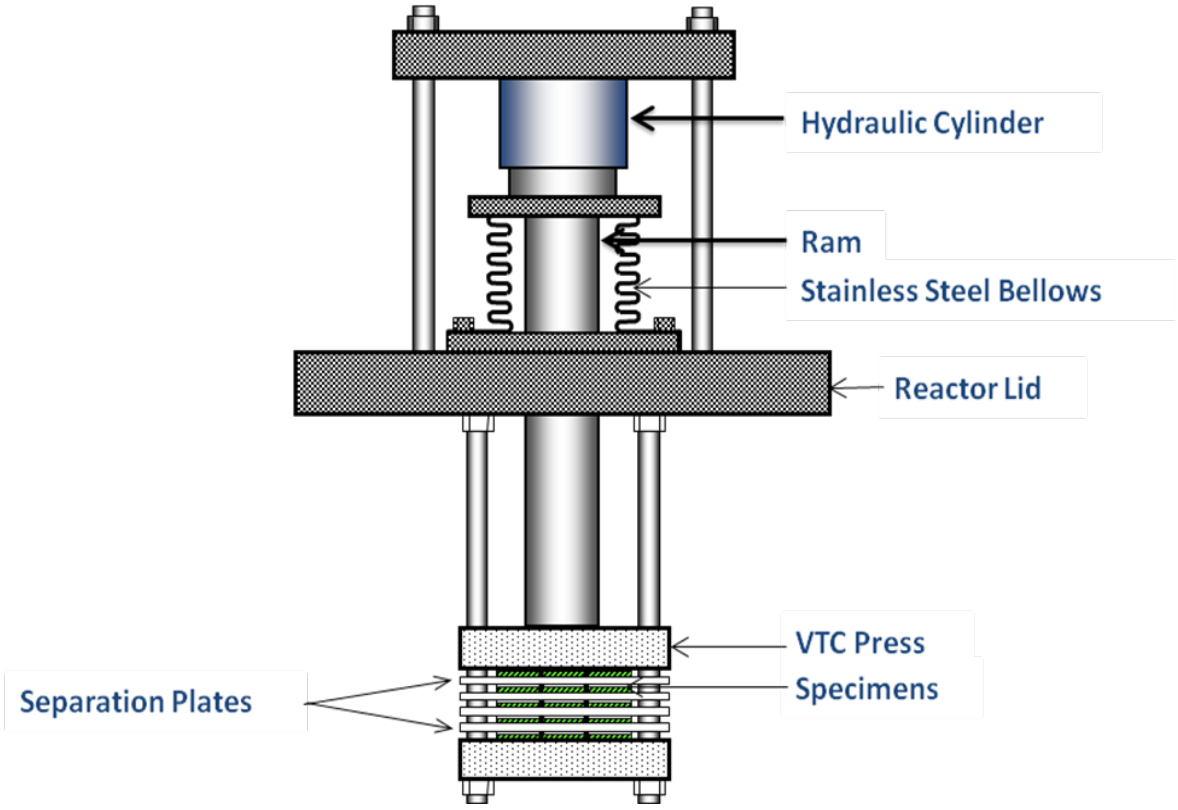

Figure 3.2.2: Side view of the multiple platen arrangement in the VTC device.

VTC is an engineered process which utilizes the heat and moisture effect on the viscoelastic polymers to the advantage of the final product. The VTC process provides first stage densification of wood in the presence of steam, which collapses the cell walls but at the same time protects the structural integrity. In this step, the polymers in the wood are softened, which aides in releasing the residual stresses. The second stage compression is done without the steam, but the wood is still soft and exhibits mechanosorptive effect. This compression adds to the dimensional stability of the VTC product and also enhances the material property. Then the sample is cooled to below 100 ºC before the mechanical pressure is removed. With this step complete fixation is achieved. Table 3.2.1 refers to the VTC schedule that was utilized.

Table 3.2.1: VTC Process Schedule.

Process Time (s)	Cumulative Time (s)	Specimen Pressure (MPa)	Platen Temp (^{o}C)	Steam Pressure (kPa)	Comments
0	0	0	>75 (<100)	0	Sample placed and lid secured
10	0	0.03	175	100	Pressurize vessel with steam
170	10	0	175	862	Conditioning- press open
120	180	1.4	175	862	1st stage compression
60	300	1.4	175	0	Discharge steam pressure
100	360	0	175	0	Specimen venting press-open
300	460	4.1 – 4.5	175	0	2nd stage compression
120	760	4.1 – 4.5	100	0	Specimen cooling
0	880	0	100	0	Open platen press

The strands that were to be processed with the VTC device had the following average dimensions: 140 x 25 x 2.3 mm (5.5 x 1 x .09 inch). These strands were not dried and were stored at -10 ºC. The density of the strands was measured before and after they went through the densification procedure. The individual VTC strands were later conditioned at 30^{o}C and 25% RH to an equilibrium moisture content of approximately 5% and then used to make the composite. Some of the VTC strands were also conditioned in the environment room (20˚C and 65% RH) to about 8-9% moisture content and then tested nondestructively to determine the MOE.

VTC wood strands, along with non-VTC strands, were used to make oriented strand composites and their mechanical properties were evaluated. Preliminary results yielded that a minimum of 20 % by weight of VTC strands were required to achieve adequate coverage of surface area to improve the bending properties of the composite. Hence the two treatments studied were composed of 20% and 40% by weight of VTC strands that were oriented on the surface. The panel size was 61 x 61 x 1.3 cm (24 x 24 x ½ inch) and target density was 585 Kg/m^3 (36 pcf). The list of treatments is shown in Table 3.2.2

Table 3.2.2: Experimental design for OSC. All core layers were randomly oriented. Number of replications for each treatment: 3.

Description	Treatment	VTC Content (weight %)	Surface Orientation (weight %)
Control (*Random Orientation*)	**A**	0	0
Reference (Oriented) 20% by weight *(No VTC strands)*	**B**	0	20
Test (Oriented) 20% by weight *(VTC strands)*	**C**	20	20
Reference (Oriented) 40% by weight *(No VTC strands)*	**D**	0	40
Test (Oriented) 40% by weight *(VTC strands)*	**E**	40	40

Three replications of a control panel (Treatment A) with no VTC strands and random orientation were prepared. There were also three replications for each treatment of a reference panel (Treatment B and D) made with no VTC strands, but surface strands oriented with two weight percentages: 20% and 40%. These were followed by three replications for each treatment of the test panel (Treatment C and E) made with VTC strands, with surface strands oriented with two weight percentages: 20% and 40%. A total of

15 panels were made and tested for bending MOE and MOR, thickness swell, internal bond and vertical density profile (VDP).

The non-VTC strands that were used to make the composite had the following average dimensions: 152 x 25 x 0.6 mm (6 x 1 x .025 inches). The strands were dried in laboratory scale dryer to about 2% – 3% moisture content. These strands were mixed with 20% and 40% by weight of VTC for the test composites. The mixture of strands was then blended with 4% resin solids based on oven-dry weight. The resin employed to make the composite was a commercial, phenol-formaldehyde, OSB face resin (48% solids content). Blending was performed in a 1.8 m (6-foot) diameter rotating blender that was equipped with a spinning disk atomizer. After blending, the VTC strands and non-VTC strands were visually separated. Identification of VTC strands was aided by color marking them prior to blending. The mats were hand-formed in a wood forming frame. In the test panels, and some control panels, the surface layers were carefully oriented and the core was randomly oriented, as indicated in the experimental design given in Table 3.2.2. The platen temperature was set at 180˚C. The schedule used to make the strand composite is illustrated in Table 3.2.3.

Table 3.2.3: Hot press schedule to make the oriented strand composite. Platen temperature was 180 ^{o}C.

Step	Time (s)	Position (cm)	Rate (cm/s)
0	0	15.2	
1	10	15.2	0.000
2	40	2.5	0.424
3	55	1.1	0.130
4	470	1.1	0.000
5	520	1.2	-0.003
6	580	15.2	-0.241
7	610	15.2	0.000

The panels were then cut according to the cutting diagram showed in Figure 3.2.3. The cut sections were then conditioned at 20^{o}C and 65% RH until equilibrium moisture content was obtained. The procedures and methods described in ASTM D 1037 were followed to test the specimens for modulus of elasticity (MOE), modulus of rupture (MOR), internal bond (IB) and thickness swell (TS). Even the vertical density profile of the samples was measured to understand better the increase in the MOE while keeping the panel density constant. The density profile measurement was based upon x-ray attenuation (Quintek Measurements Model QDP-01X Vertical Density Profiler). Static 3-point bending test was performed until failure to measure the MOE and MOR using a Sintech universal testing machine.

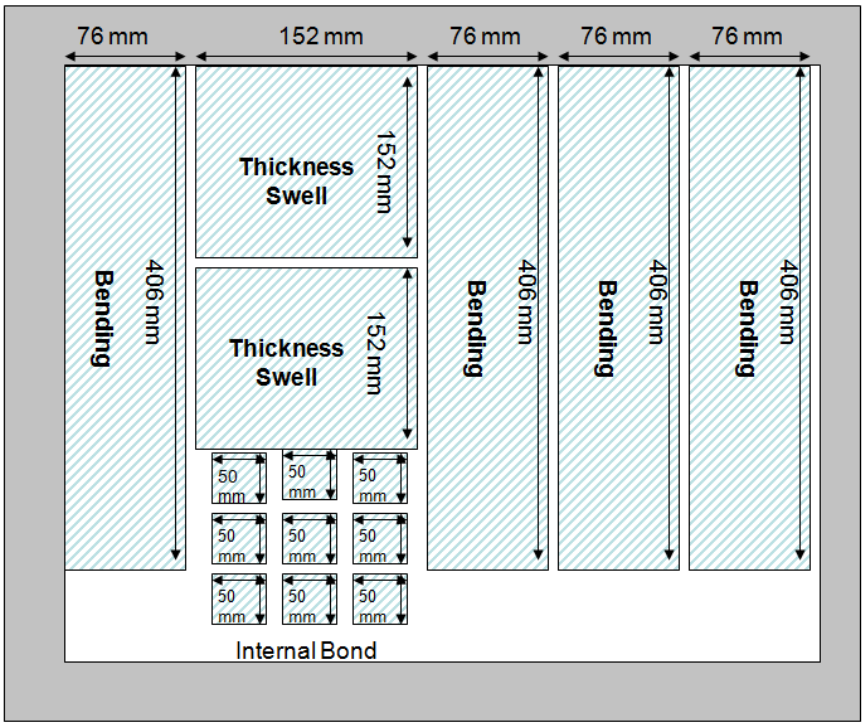

-Not to scale

-The samples were cut at least 2 inches from the rough edges.

Figure 3.2.3: Cutting pattern for OSC.

3.3 VTC composite

The modified VTC device was used to process wood strand composites. A total of 9 random-oriented strand boards with dimensions: 91 x 91 x 0.6 cm (36 x 36 x ¼- inch) were produced in the laboratory for the study. These boards were then cut according to the cutting diagram shown in Figure 3.3.1. The strands that were used to make the random-oriented strand board had the following average dimensions: 152 x 25 x 0.6 mm (6 x 1 x .025 inches). The strands were dried in laboratory scale dryer to about 2% – 3% moisture content. The dried strands were then blended with 4% resin solids based on oven-dry

weight. The resin employed to make the composite was a commercial, phenol-formaldehyde, OSB face resin (48% solids content). Blending was performed in a 1.8 m (6-foot) diameter rotating blender that was equipped with a spinning disk atomizer. After blending, the mats were hand-formed in a wood forming frame. All the strands were randomly oriented while forming the mat. The platen temperature was set at 180˚C. The schedule used to make the strand composite is illustrated in Table 3.3.1.

Table 3.3.1: Hot press schedule to make the strand composite. Platen temperature was 180^{o}C.

Step	**Time (s)**	**Position (cm)**	**Rate (cm/s)**
0	0	15.2	
1	10	15.2	0.000
2	40	2.5	0.424
3	55	0.6	0.130
4	470	0.6	0.000
5	520	0.7	-0.003
6	580	15.2	-0.241
7	610	15.2	0.000

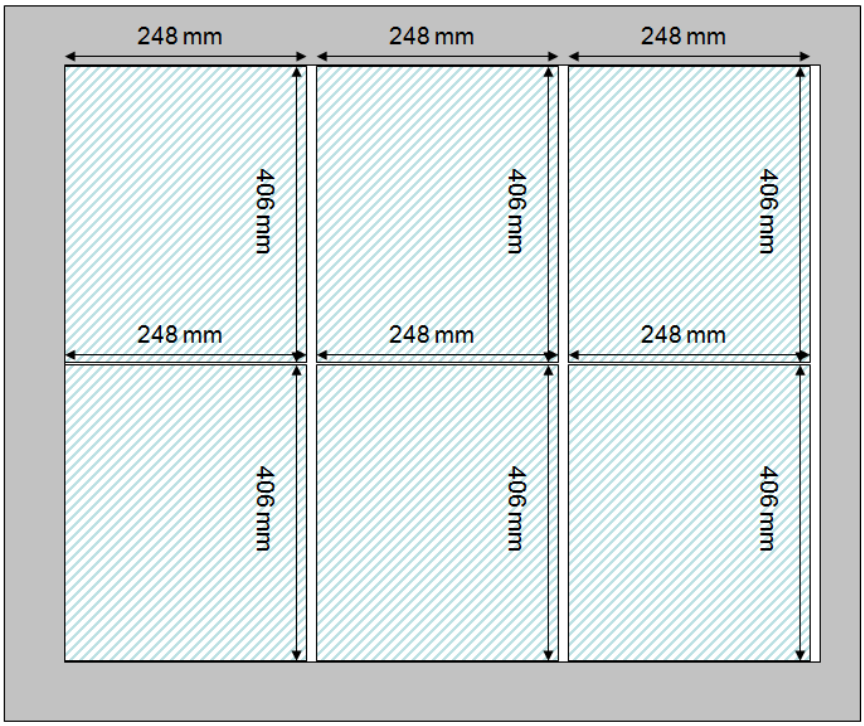

Figure 3.3.1: Cutting pattern for strand composite that was modified by the VTC process.

The strand board was compressed to three different target degrees of densification: 122%, 94% and 71% based on the initial density. Four replications were made for each degree of densification. The panels were 41 cm (16-inch) long and 25 cm (10-inch) wide and conditioned at 20 ºC and 65% RH until equilibrium moisture content was obtained. Two VTC lamina were bonded to one core non-VTC lamina to create a 3-layer composite. Two types of phenol-formaldehyde resin, and their method of application, were tested to determine a suitable adhesive system. The best method consisted of application of two different phenol-formaldehyde (PF) resins. Commercially available PF OSB face resin (48% solids) was applied to VTC lamina. A structural plywood phenol-formaldehyde resin

(36.5% solids) was applied to the non-VTC lamina. Both the resins were obtained from Georgia Pacific Resins Inc. The total amount of resin solids that was applied upon the laminas was 0.122 Kg/m^2 (0.025 lb/ft^2), with half applied to each surface of the bondline.

The three layered composite was subjected to the following hot press schedule. Initially, the composite underwent 5 minutes of pressing at 1.03 MPa (150 psi). Then the pressure was reduced to 1/3 of the initial pressure and the press time for this pressure was 4 minutes and 30 seconds. Also a 30 second vent time was provided to slowly reduce the pressure to avoid blow outs in the panel. The platens were kept at 150 ºC so as to achieve reduced steam pressure at the bondline.

Density of the individual VTC, non-VTC lamina, and the composite was determined at each stage. Nondestructive tests were performed on the non-VTC lamina and VTC lamina to determine the MOE prior to 3-layer composite manufacture. MOE and MOR of the VTC modified laminated strand composite was determined as well.

3.4 Statistical Analysis

Statistical analysis for this project was completed using the available S-plus version 7.0 and SPSS. The goal of this analysis was to statistically determine the significant differences in properties obtained from different treatments using analysis of variance (ANOVA) method. The relation between densification and mechanical properties was analyzed using both

linear and non-linear regression fitting methods. The sample size are defined in the test matrices given below in Table 3.4.1 and Table 3.4.2.

Table 3.4.1: Test matrix containing the sample sizes for the influence of VTC wood strands on the OSC.

Treatments	**Bending**	**Internal Bond**	**Thickness Swell**	**Vertical Density Profile.**
A	12	27	6	27
B	12	27	6	27
C	12	27	6	27
D	12	27	6	27
E	12	27	6	27

Table 3.4.2: Test matrix containing the sample sizes for the strand composite that was modified by the VTC process.

Degree of Densification (%)	**Sample Size**
122	4
94	4
71	4

Chapter 4: Results

4.1 Construction of a VTC device to process oriented strand composites.

The scaleup VTC device was constructed as such to process samples that were 61 cm (24 inch) in length and 25 cm (10 inch) in width compared to the previous device which produced samples of dimension 15 cm by 5 cm (6-inch by 2-inch). A schematic representation of the device is shown in Figure 4.1.1.

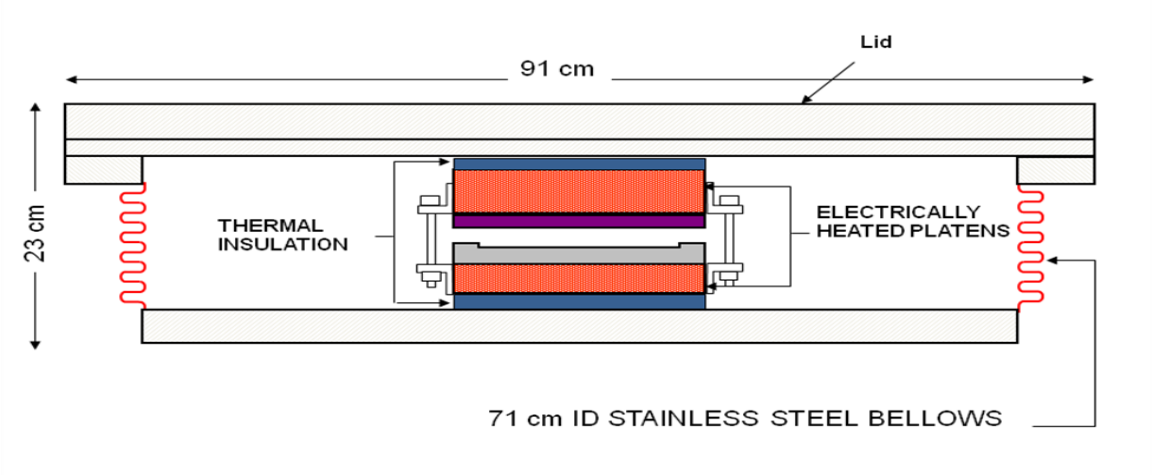

Figure 4.1.1: Schematic (side view) of the constructed VTC device.

The lid consists of several ports to be used for various puposes. Some of which includes: cooling water inlet and outlet, electrical lines into the device, thermocouple wires, water in for steam generation, steam vent and safety valve. The detailed description is depicted in Figure 4.1.2. The platens in the setup were made from 3.8 cm (1.5 inch) thick aluminum. They were equipped with 1.3 cm (½ inch) diameter holes to provide cooling water lines and

ports for heating elements. A total of five electric heating elements were installed in a single platen. Also, there was a 3 mm (1/8 inch) diameter hole, centered upon the thickness and width of platen to contain the thermocouple. Schematic representation of the platen is shown in Figure 4.1.3. The temperature of the internal top and bottom platens were independently controlled by a proportional loop controller.

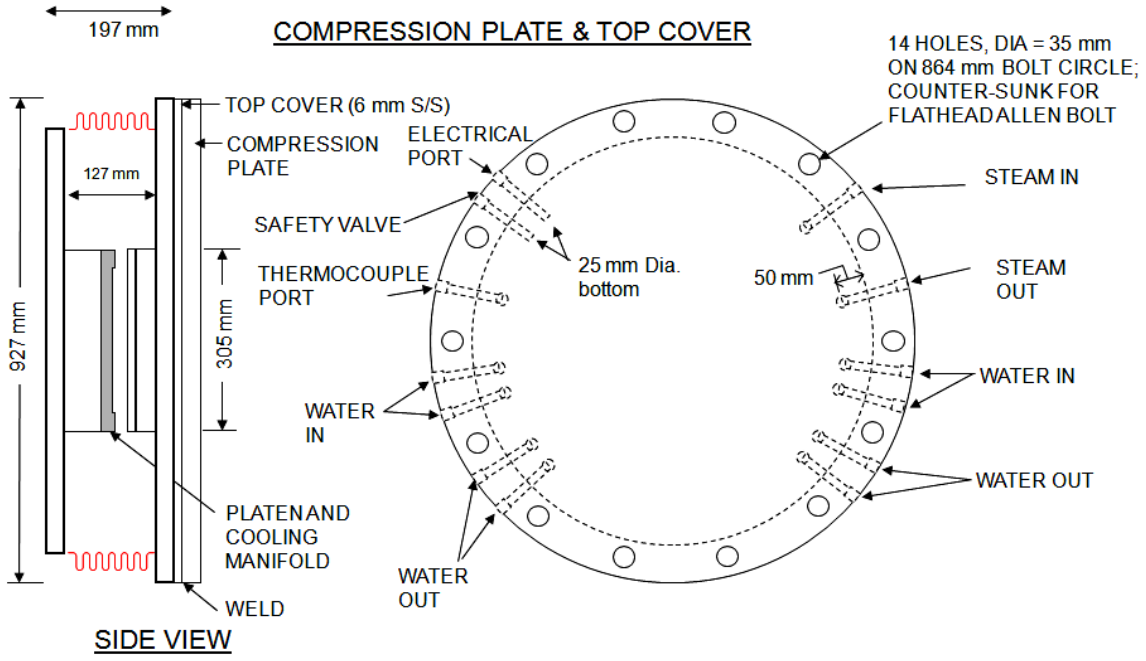

Figure 4.1.2: Top and side view of the compression plate and top cover.

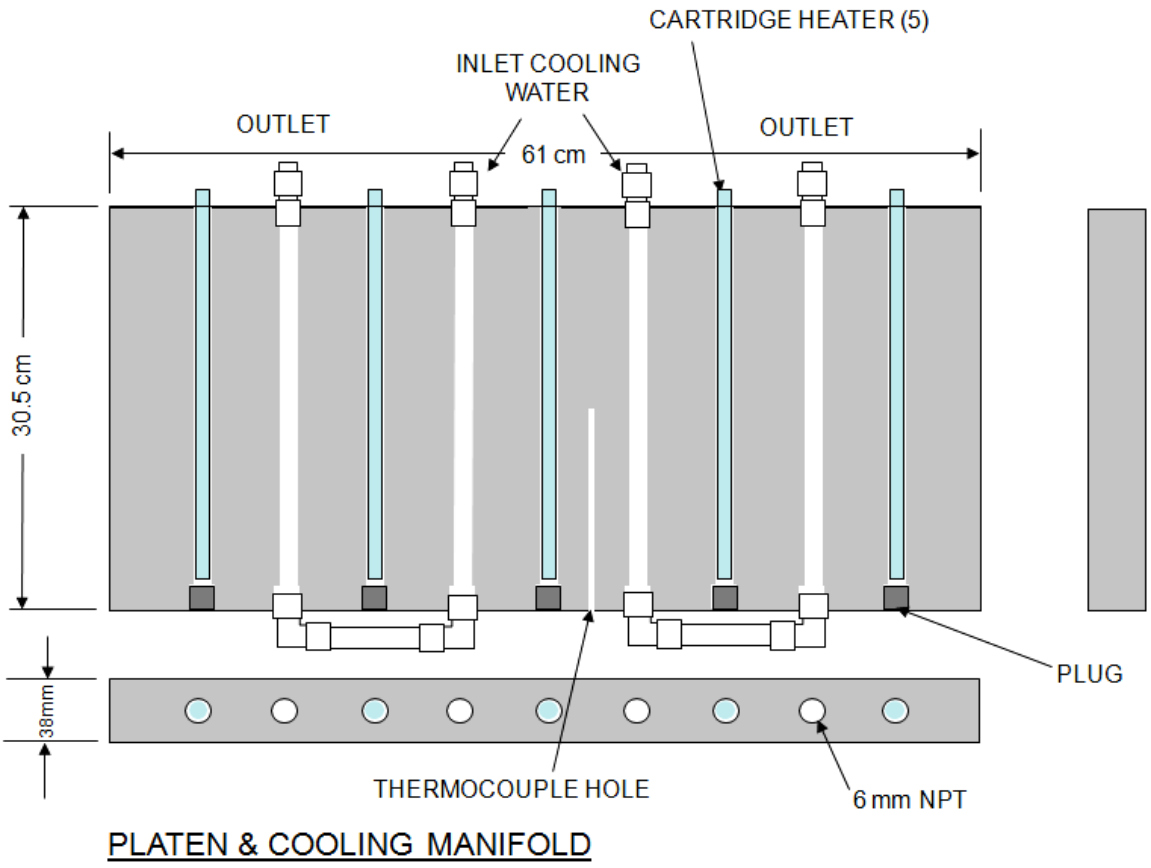

Figure 4.1.3: Platen assembly showing cooling and heating setup.

External plumbing lines, as described in Figure 4.1.4, were installed for the following purposes: pump water into the device for steam generation, steam vent, cooling water inlet and cooling water outlet. The lid when opened shows the device from inside and this is shown clearly in the photographic image in Figure 4.1.5.

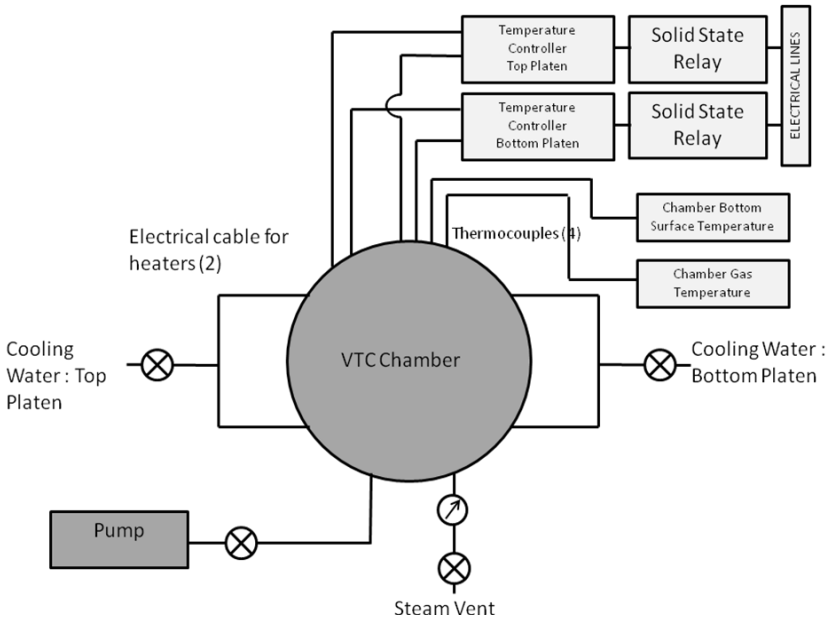

Figure 4.1.4: Steam and valve assembly.

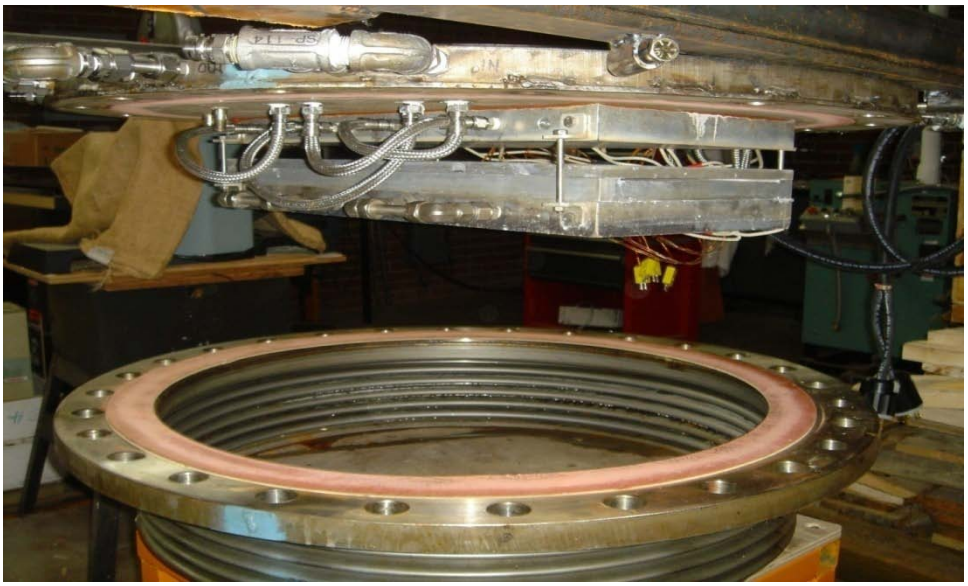

Figure 4.1.5 VTC device shown with the lid opened. Independently-heated platens are attached to the inside of the lid.

The operating schedule of the device was configured after multiple trial and error runs. Manipulating of a few factors and some mechanical changes helped achieve a consistent schedule that was used to process the samples. Firstly, the device was preheated until the inside bottom surface of the bellows reached 200˚C. This was accomplished with a setpoint temperature of the hot-press platens of 240˚C. Then the device was taken out of the hot press, the sample was placed inside the vessel, lid secured and the device was positioned back into the hot press. This was a time consuming process and created variability in the thermal history of the samples. The schedule described in Table 4.1.1 was then followed to make the test specimens.

Table 4.1.1. VTC process schedule.

Process Time (s)	**Cumulative Time (s)**	**Setpoint Position (mm)**	**Platen Temp (^{o}C)**	**Steam Pressure (kPa)**	**Comments**
0	0	215	>75 (<100)	0	Sample placed and lid secured
400	0	215	175	100	Pressurize vessel by injection of water
180	400	207.1	175	862	1st stage compression
60	580	207.1	175	0	Discharge steam pressure
60	640	215	175	0	Specimen venting press-open
450	500	202.8	200	0	2nd stage compression and wait till the average platen temperature reaches 200˚C
360	950	202.8	120	0	Specimen cooling
0	1310	215	120	0	Open platen press

The platens inside the device were equipped with springs to provide a gap between the top of the sample and the bottom of the upper platen during the conditioning phase. This allowed intimate contact between the sample and the environment. The steam in the device was produced in situ by adding a known quantity of water, which was calculated using the ideal gas law for saturated steam at a known temperature and volume. Extra water was added, due to variable temperature and condensation on internal surfaces. Initially a flow of water by gravity was chosen, but the initial insertion of water developed enough steam pressure to off-set the force of gravity and prevents some of the water from entering the device. A piston pump was added to make sure the water was inserted into the system. Also, thermal insulation was added to the outside of the flexible bellows to minimize condensation of steam within the vessel and maintain a constant temperature.

4.2 Influence of VTC wood strands on the mechanical properties of an oriented strand composite.

The density of a wood species is a prime factor that determines the mechanical properties, such as MOE and MOR (Hoadley 2000, USDA 1999). It is also known that the vertical density profile that normally develops in OSC products as a result of hot-pressing contributes to bending properties. Typically the surface layer has a greater density than the core. This section outlines how this concept was engineered to increase the mechanical property of an OSC composite while keeping the overall density constant. This was achieved by using high density VTC strands that were aligned on the surface of a wood strand composite.

The theory of simple mechanics states that the maximum tensile and compressive stresses, when a beam is subjected to bending, are on the surface. Hence, if the tensile and compression properties in the surface of a laminated beam are increased, then the overall bending properties of the beam will be improved. This concept is applied in the manufacturing of the OSC with the addition of VTC strands. It can thus be inferred that the inclusion of the high density VTC strands in the face layers of the three-layered composite will improve the bending strength and stiffness of the product.

The strands that were to be processed with the VTC device had the following nominal initial dimensions: 140 x 25 x 2.3 mm (5.5 x 1 x .09 inch). The target density for the densification

was set to be 1 g/cm^3, but the achieved density was only 0.91 g/cm^3, with an average thickness of 1 mm (0.04 inches). The density was calculated using dry weight basis and dimensions right after VTC processing. Furthermore, it was assumed that the samples had about 0% moisture content immediately after VTC processing. Some of the VTC strands were also conditioned in the environment room at 20˚C and 65% RH until constant moisture content was attained and then tested nondestructively to determine the MOE. It was found that the average MOE increased 103% and the observed increase in density was found to be 133%.

Table 4.2.1. Density and MOE of wood strands before and after VTC processing. Specimens conditioned at 20^{o}C and 65% RH.

Description		**Standard Test Procedure**	**Number of replications**	**Mean**	**Standard Deviation**
Density (g/cm^3)	Before VTC	-	244	0.39	0.0628
	After VTC		244	0.91	0.1050
MOE (GPa)	Before VTC*	ASTM D 1037	30	9.5	0.001
	After VTC*		30	19.3	0.004

*Samples before VTC and after VTC were different, which resulted in variable results.

Two treatments were studied that were comprised of 20% and 40% by weight of the total amount of strands required for OSC production. The target panel size was 61 x 61 x 1.3 cm (24 x 24 x ½ inch) and target density was 585 Kg/m^3 (36 pcf). Deviation from the target

density occurred in individual test specimens because of local variability in mat formation across the length and width. In addition, each treatment appeared to yield a different degree of springback upon removal of the panel from the hot-press. The difference in density is illustrated in Table 4.2.2. It is clearly observed that the density increases as we increase the weight percentage of oriented strands on the surface. This was likely due to the mat forming procedure where placement of the oriented strands was more precise than random oriented strands inside of the forming frame. For the above mentioned reasons, inclusion of density as a covariate in the statistical analysis was important.

Prior to starting the statistical analysis it was observed that one panel in the treatment with 40% normal strands oriented on the surface had high variability in thickness swell values. It was then realized that one of the panels (corresponding to 4 thickness swell samples) had very high thickness swell (2hr) of the order of 14% compared to the other two panels whose average thickness swell (2hr) was only about 5%. Visual analysis didn't reveal anything unusual within the samples, but, this panel alone was manufactured a week later than the others. Also, during blending with resin, only two-thirds of the normal amount of strands (enough to make two panels instead of three) was placed in the blender. Perhaps this resulted in less resin coverage on the strands and more resin lost in the blender. Lesser resin would then explain the very high thickness swell in that panel alone. An ANOVA was performed within the treatment and it was found that one panel had statistically significant different result compared to the others. This evidence was strong enough to exclude all data for this panel from the study and then perform the final statistical analysis.

The bending properties increased dramatically just with orientation of strands on the surface. Panels with 20% and 40% by weight of normal strands (no VTC strands) oriented on the surface showed a dramatic increase in the MOE, by 55% and 64%, and MOR, by 22% and 33%, respectively. Inclusion of VTC strands resulted in an increase in the flexural properties but the increase was not as striking as that shown by orientation. Panels with 20% by weight of VTC strands oriented on the surface increased the MOE and MOR by 6% and 8%, respectively, with respect to their control, which was 20% orientation of normal strands on the surface. The addition of 40% VTC strands improved the MOE and MOR by 30% and 18%, respectively. It was observed while forming the mat with 20% by weight of VTC strands that the VTC strands didn't form a continuous layer on the surface. Furthermore, the bending test samples revealed that the failure mostly occurred either between the interface of normal and VTC strands or in the non-continuous layer. With the incorporation of 40% by weight of VTC strands, an uninterrupted surface was achieved, resulting in a statistically significant increase of MOE and MOR. The box plots of the MOE and the MOR values are illustrated in Figure 4.2.1 and Figure 4.2.2. In Figure 4.2.1 it was visually observed that treatments D and E were different and they were expected to have statistically significant differences. Whereas, in Figure 4.2.2 the MOR values seemed to increase from treatment A to E but less significant observations were drawn.

Table 4.2.2. Mean density data and flexural properties of the treatments. Total number of replications for individual treatments was 12.

Description	**Density (Kg/m^3)**		**MOE (GPa)**		**MOR (MPa)**	
	Mean	**SD**	**Mean**	**SD**	**Mean**	**SD**
Control (Random Orientation)	580.9	28.0	7.6	1.0	49.3	7.4
Control (Oriented) 20% by weight *(No VTC strands)*	595.1	41.8	11.7	1.6	60.1	9.2
Test (Oriented) 20% by weight (VTC strands)	631.8	43.1	12.4	1.7	64.9	9.3
Control (Oriented) 40% by weight (No VTC strands)	643.8	23.6	12.4	0.7	65.5	10.2
Test (Oriented) 40% by weight (VTC strands)	666.9	43.9	15.9	2.5	77.1	7.6

It was observed that the mean internal bond values decreased by 4% and 6% with the addition of 20% and 40% VTC strands. However, there was no statistically significant difference ($\alpha = 0.05$) in the internal bond strength values between the treatments. This is visually observed in Figure 4.2.3. The thickness swell values, on the other hand, varied with the inclusion of the high density strands. With the inclusion of 20% VTC strands, the average thickness swell values after 2 hour, 24 hour and redried values increased by 52%,

25% and 14%, respectively. Statistical analysis ($\alpha = 0.05$) provided evidence that there is significant difference after the 2-hour soak period, but not for the other levels. Addition of 40 % VTC strands increased the thickness swell values for the 2-hour, 24-hour and redried periods by 155%, 56% and 38%, respectively. Statistical analysis yielded that there is significance difference for the thickness swell values after 2-hour soak and 24-hour soak. A very obvious trend of increase in the thickness swell can be observed with the addition of extra 20% VTC strands. This makes sense as there were higher numbers of VTC strands on the surface. It is visually evident from the box plot of the thickness swell values in Figure 4.2.4, Figure 4.2.5 and Figure 4.2.6, that there is a lot of variability in the values which can be attributed to the horizontal density distribution in the panels.

Table 4.2.3. Mean internal bond and water-soak thickness swell data for the treatments. Total number of replications for IB was 27 and for thickness swell was 6.

Description	**IB (kPa)**		**Thickness Swell (%)**					
	Mean	**SD**	**2 hour**		**24 hour**		**Redried**	
			Mean	**SD**	**Mean**	**SD**	**Mean**	**SD**
Control *(Random Orientation)*	731.7	128.7	7.30	0.77	19.53	1.97	14.83	3.13
Control (Oriented) 20% by weight *(No VTC strands)*	764.1	121.3	6.79	1.82	18.73	3.20	16.16	3.57
Test (Oriented) 20% by weight *(VTC strands)*	731.4	121.7	10.33	3.98	23.45	4.15	18.37	6.42
Control (Oriented) 40% by weight *(No VTC strands)*	846.1	159.6	4.3	1.12	15.37	2.07	12.63	2.51
Test (Oriented) 40% by weight *(VTC strands)*	766.5	208.9	10.97	2.33	23.97	0.66	17.40	1.98

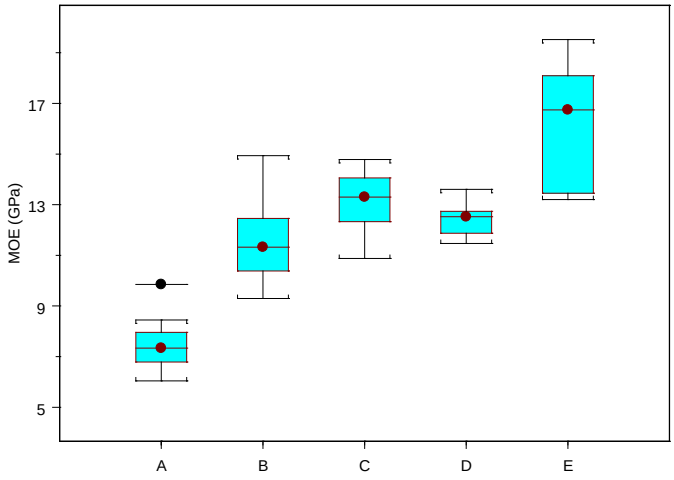

Figure 4.2.1 Box plot of the MOE values of five treatments of the oriented strand composite. Plot shows median, upper and lower quartiles, and maxima and minima excluding outliers.

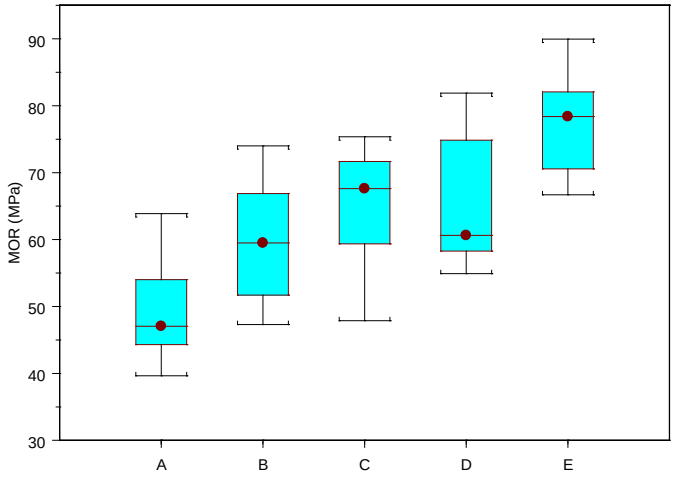

Figure 4.2.2 Box plot of the MOR values of five treatments of the oriented strand composite. Plot shows median, upper and lower quartiles, and maxima and minima excluding outliers.

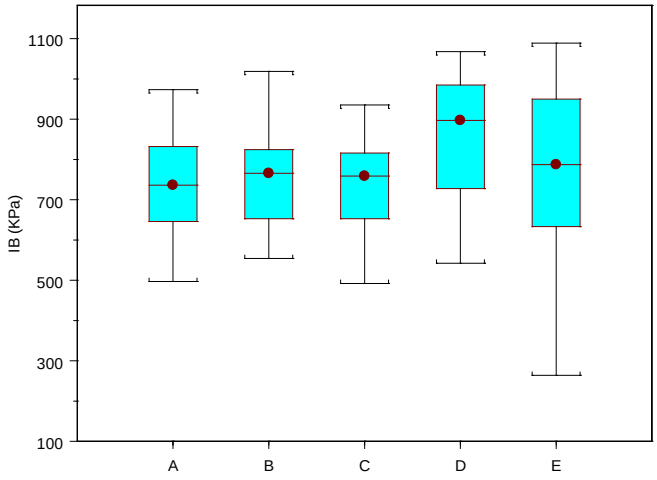

Figure 4.2.3 Box plot of the internal bond values of five treatments of the oriented strand composite. Plot shows median, upper and lower quartiles, and maxima and minima excluding outliers.

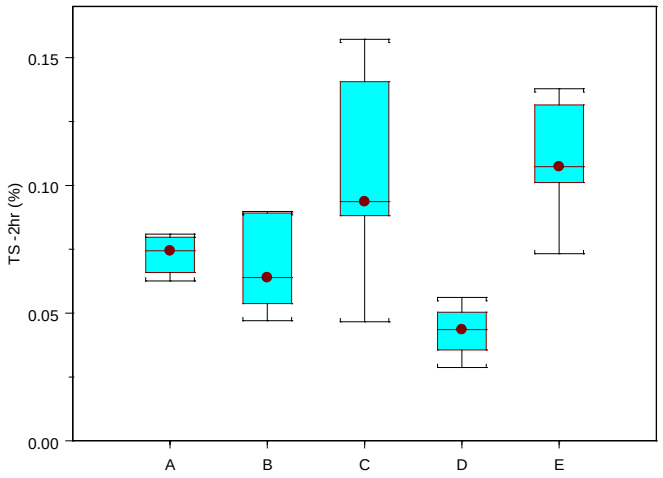

Figure 4.2.4 Box plot of the thickness swell (2 hr) values of five treatments of the oriented strand composite. Plot shows median, upper and lower quartiles, and maxima and minima excluding outliers.

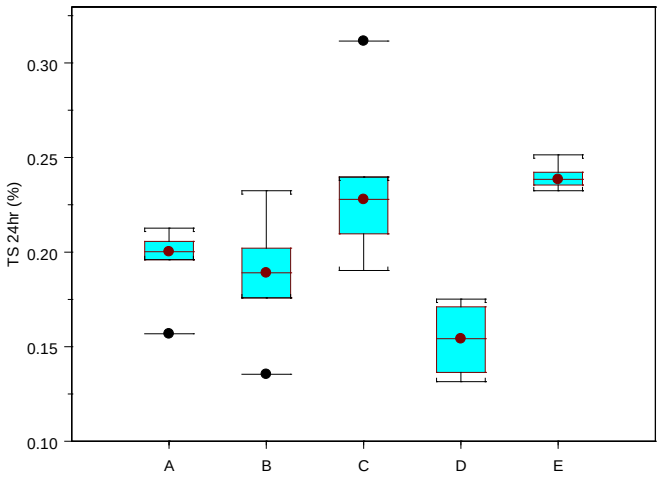

Figure 4.2.5 Box plot of the thickness swell (24 hr) values of five treatments of the oriented strand composite. Plot shows median, upper and lower quartiles, and maxima and minima excluding outliers.

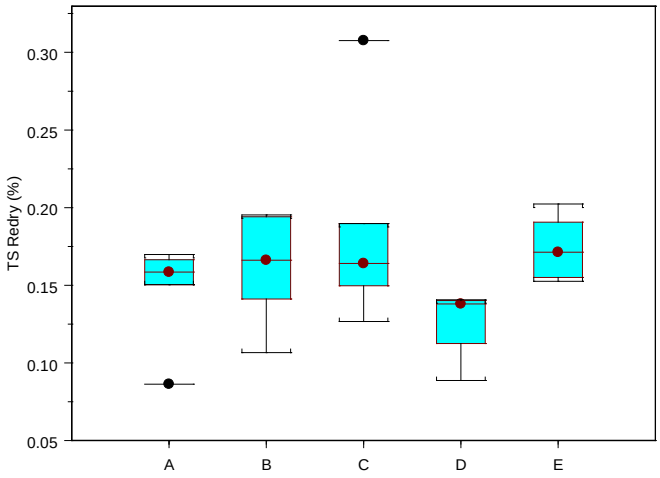

Figure 4.2.6 Box plot of the thickness swell (redried) values of five treatments of the oriented strand composite. Plot shows median, upper and lower quartiles, and maxima and minima excluding outliers.

The fundamental reasoning, that would clearly explain the increase in the flexural properties, would be defined by the vertical density profiles of the samples from the treatments. The vertical density profiles of the five different treatments are illustrated in Figure 4.2.7, Figure 4.2.8, Figure 4.2.9, Figure 4.2.10 and Figure 4.2.11. Careful analysis of the treatment with 20% inclusion of VTC strands yielded that there was no significant increase in the surface densities compared to its control. However, with 40% addition of VTC strands on the surface, the density didn't quite increase as much as its control, but the thickness of the high density surface layer was higher. Hence, the thicker high density region on the face layers in treatment E, compared to the thinner high density regions in the face layer in treatments A, B and D, explains to some extent the significant increase in the flexural properties.

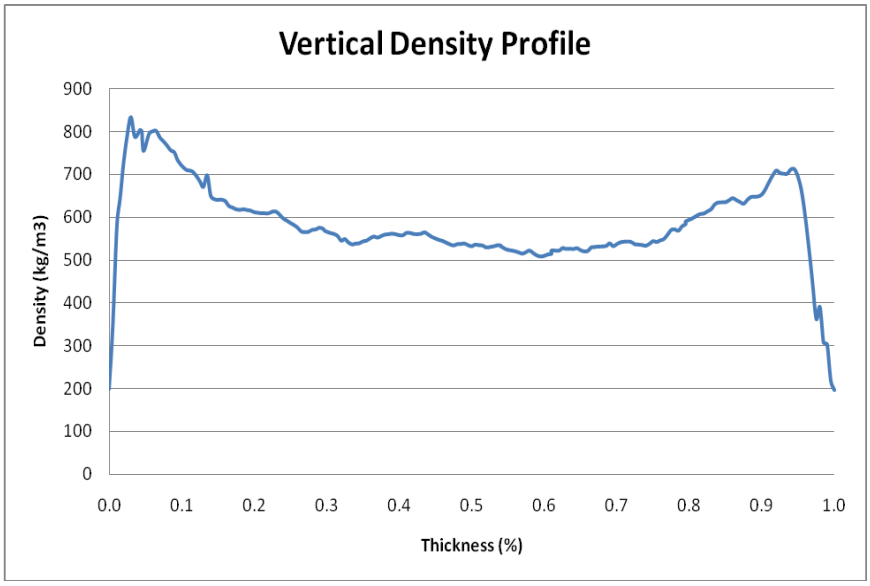

Figure 4.2.7: Averaged vertical density profiles of 8 control specimens with complete random orientation (Treatment A).

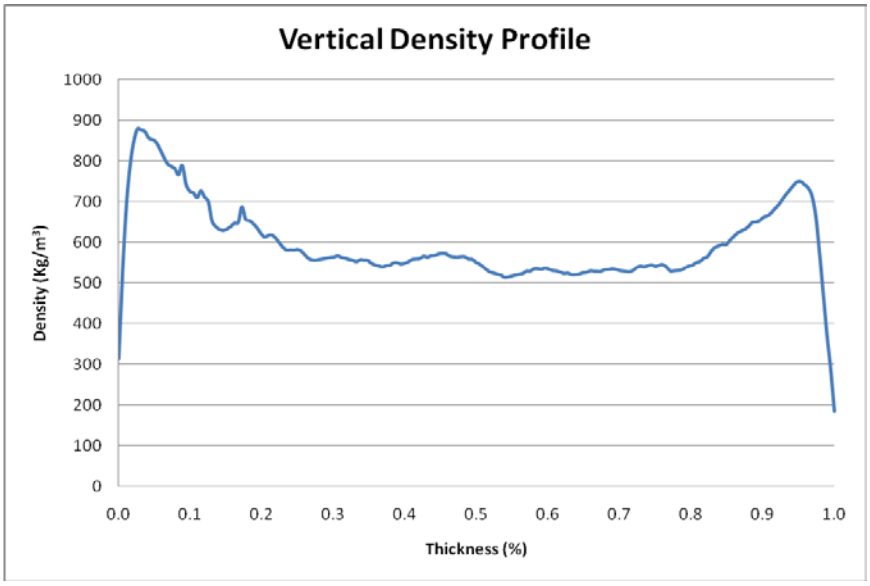

Figure 4.2.8: Averaged vertical density profiles of 8 control specimens with 20% (by weight) of normal strands, oriented on the surface (Treatment B).

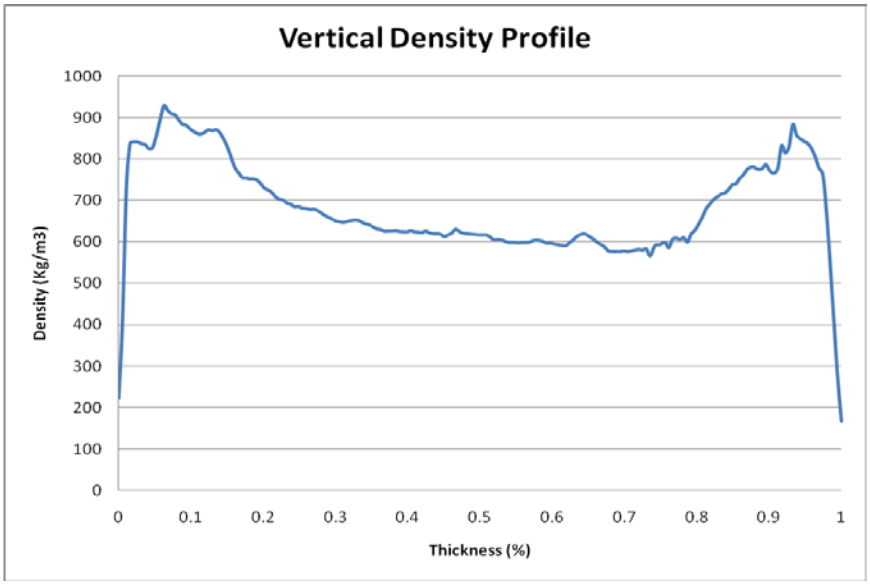

Figure 4.2.9: : Averaged vertical density profiles of 8 specimens with 20% (by weight) of VTC strands, oriented on the surface (Treatment C).

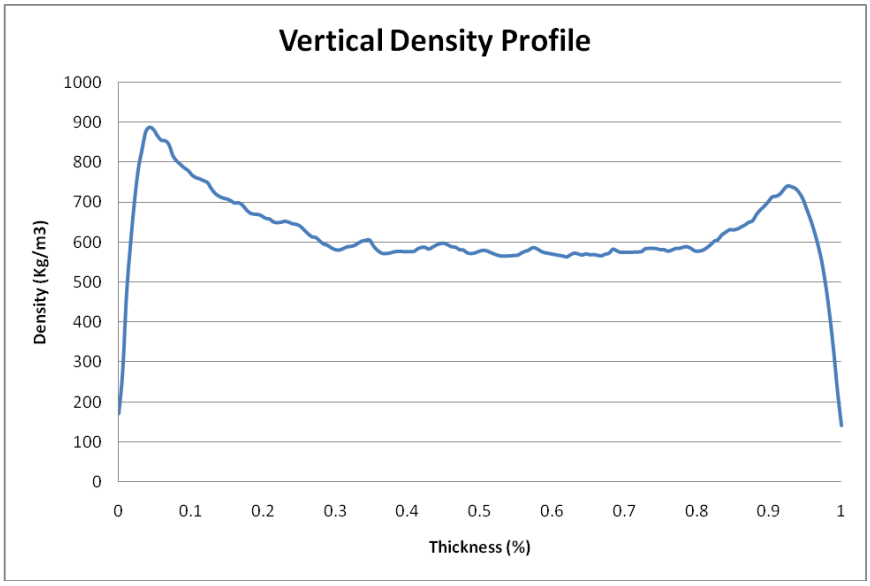

Figure 4.2.10: Averaged vertical density profiles of 8 control specimens with 40% (by weight) of normal strands, oriented on the surface (Treatment D).

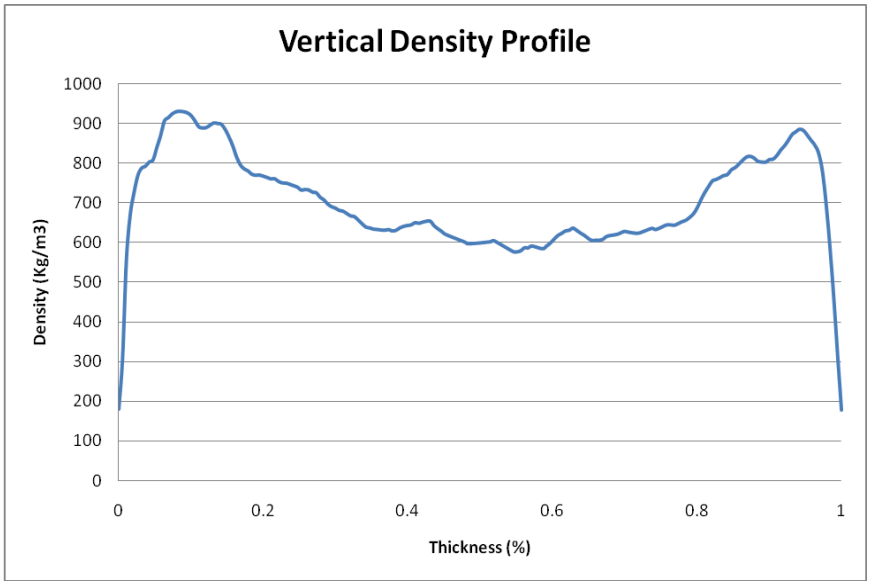

Figure 4.2.11: Avergaed vertical density profiles of 8 specimens with 40% (by weight) of VTC strands, oriented on the surface (Treatment E).

4.3 Mechanical properties of an oriented strand composite that has been modified by the VTC process.

The laboratory manufactured 6 mm (¼ inch) strand board was subjected to VTC processing and the density increased. Three different target densification levels were set: 122%, 94% and 71% with four replications each. Previous VTC runs have indicated potential cell wall failure in the wood specimen if the density was increased beyond 1.4 g/cm^3 (87 pcf), which is the approximate density of the wood cell wall. This approach was the primary factor which decided the three different treatment levels. The density and the MOE of the strand composite before and after VTC processing are illustrated in Table 4.3.1. Bending tests were only done within the elastic range because the VTC laminas were to be used to manufacture 3-layer VTC composites.

It was observed from Figure 4.3.1 that the increase in wood strength and stiffness was higher than the increase in wood density for each of the densification levels. Percentage increases in the average density and MOE for the highest target densification were found to be 109% and 158%. The increases for the mean density and MOE achieved with the median target densification were found to be 95% and 162%. Similarly, for the lowest target densification level, the average density and MOE were enhanced by 101% and 152%. There was variability observed in the MOE values (see Figure 4.3.1, Figure 4.3.2, Figure 4.3.3). The variability can be ascribed to variability in mat formation and also to the manufacturing stages of the strand composite.

Table 4.3.1. Properties of densified strand composite before and after VTC process (4 replications for each treatment). Specimens conditioned to 20˚C and 65% RH.

Target Densification Level (%)	**Description**		**Mean**	**Standard Deviation**
122	**MOE (GPa)**	Before VTC	3.32	0.74
		After VTC	8.54	2.07
	Density (Kg/m^3)	Before VTC	503.8	40.6
		After VTC	1053.0	84.5
94	**MOE (GPa)**	Before VTC	3.87	0.62
		After VTC	10.16	0.48
	Density (Kg/m^3)	Before VTC	559.0	69.9
		After VTC	1092.0	19.5
71	**MOE (GPa)**	Before VTC	3.49	0.44
		After VTC	8.80	1.45
	Density (Kg/m^3)	Before VTC	500.5	29.3
		After VTC	1007.5	32.5

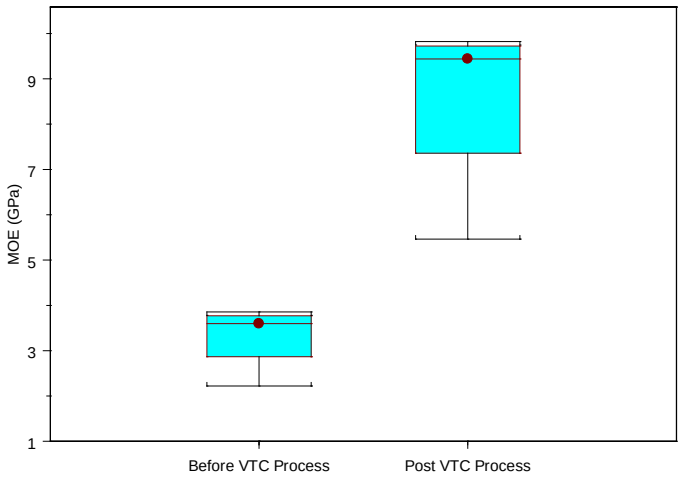

Figure 4.3.1. Box plot of the MOE values before and after VTC processing for 122% densification level. Plot shows median, upper and lower quartiles, and maxima and minima excluding outliers.

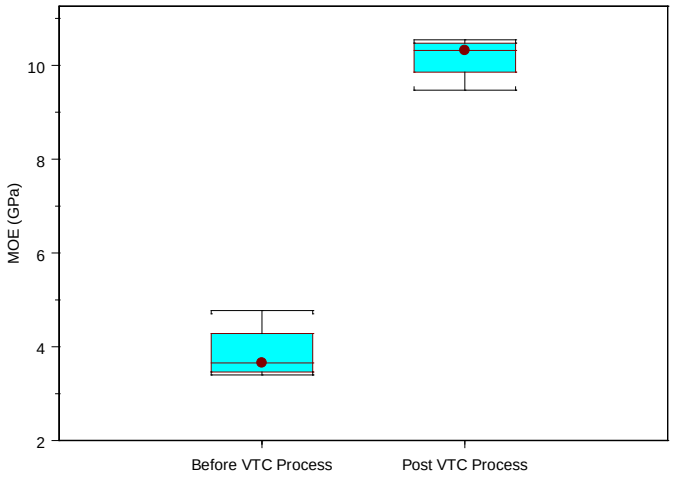

Figure 4.3.2: Box plot of the MOE values before and after VTC processing for 94% densification level. Plot shows median, upper and lower quartiles, and maxima and minima excluding outliers.

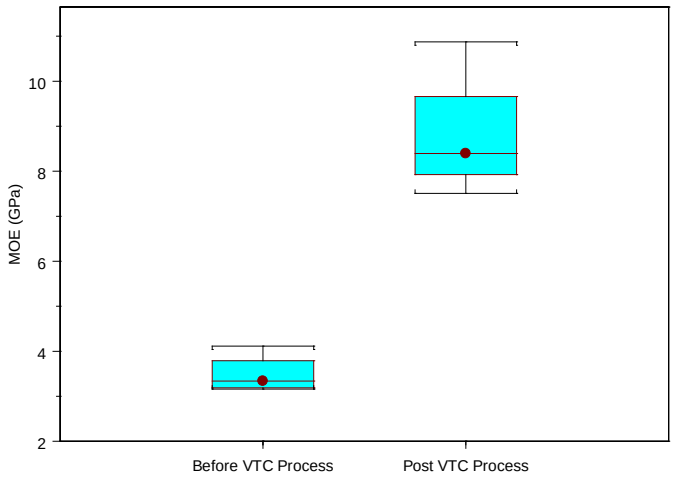

Figure 4.3.3: Box plot of the MOE values before and after VTC processing for 71% densification level. Plot shows median, upper and lower quartiles, and maxima and minima excluding outliers.

After statistical analysis it was observed that treatments were not significantly different from one another in regard to actual density after the VTC process. There was a statistically significant difference between the MOE values before and after VTC processing of the strand board ($\alpha = 0.05$). The inability to achieve different density levels will be discussed in the next chapter.

The three layered composites were tested for bending until failure to determine the strength and stiffness using the ASTM D1037 standards. The average values of the bending properties are included in the summary Table 4.3.2. Figure 4.3.4 illustrates the MOE values of the three-layered composite compared with the theoretically calculated

counterparts. The theoretical computations were based on the classical lamination theory. The prime assumptions underlying the theory are: linear elastic behavior in all the layers and complete transfer of stresses across all the interfaces. It can be clearly observed in Figure 4.3.4, that the theoretical results are higher than the experimental values. This is due to the violations of the assumptions of classical lamination theory. Wood strand composites are not homogeneous. There are voids in the composite, discontinuous strand structure, and a density profile. The bondline between the three layers may not provide complete and perfect transfer of stresses through the interface.

Table 4.3.2: Properties of three layered laminate strand composite. Specimens conditioned to 20˚C and 65% RH. Number of replications for each densification level was 6 (except for the 71% target densification level where only 3 replications were studied).

Target Densification Level (%)	**Average Density (Kg/m^3)**	**Average MOE (GPa)**	**Average MOR (MPa)**
122	747.5	5.60	34.40
94	775.1	6.37	42.51
71	775.1	6.42	39.98

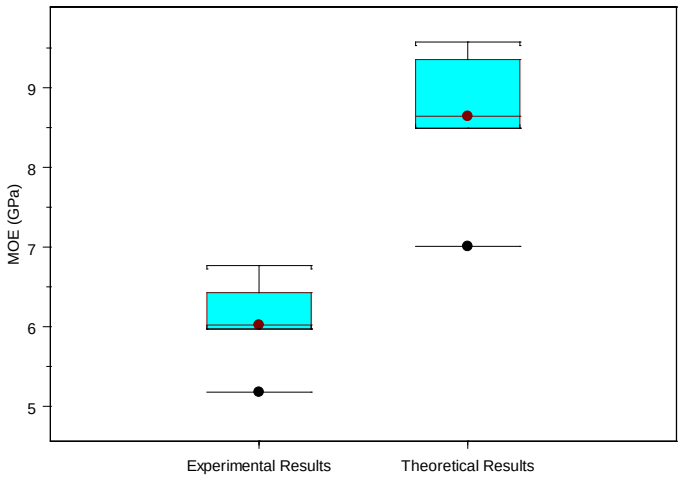

Figure 4.3.4: Box plot of the experimental and theoretically computed MOE values of the three-layered composite. Plot shows median, upper and lower quartiles, and maxima and minima excluding outliers.

Chapter 5: Discussion

5.1 Scale-up VTC device to process oriented strand composites.

The device was successfully constructed and a standard operating procedure was established. The control of the device was only semi-automated, so there was difficulty obtaining repeatable process conditions without considerable practice. There are still some issues with the device that have to be solved, and some modification provided, to improve the operation and performance of the system. The requirement of removing the entire chamber from the hot-press for loading and unloading specimens caused a dynamic heating and cooling situation for each run. Each run required time for the system to obtain the setpoint temperature. Since the specimens are heat sensitive, the heating time had to be as brief as possible. The independent heating elements that were installed in the top and bottom platens did not provide equal heating rate because the thermal mass was not equal. The top platen is attached to the lid, which is a large heat sink, while the bottom platen was suspended in space when no force was on the specimen. The heater controls were monitored and adjusted in an attempt to obtain an equal heating rate, but some deviation always occurred.

An important step during the VTC process is the cooling of the specimen before the compression force is released. The platens are cooled by circulating water through the platens. Equal cooling rate was again an issue, but this was controlled by adjusting the

water flow rate through the platens and carefully monitoring the platen temperature. Another issue related to cooling was condensation on the platens. At the time cooling is started the atmosphere inside the chamber is entirely water vapor. Condensation will form on any surfaces at or below the dewpoint. If liquid water contacts the sample, immediate thickness swell in the sample may occur upon removal of compression force. It was realized during the processing of some test samples that some condensation occurred on the platens, which caused thickness swell in areas of exposure. This resulted in uneven thickness across the specimen. It was first thought that the vent time was not long enough, but increasing vent time did not solve the problem. The initial cooling procedure was to reduce the platen temperature to 100^{o}C. It was decided to cool the platens to 120˚C instead of 100˚C. This insured that only vapor phase water would be present at atmospheric pressure. The glass transition temperature of wood is a function of moisture content. It can be fairly assumed that the moisture content of the specimen during the second stage compression is very close to 0% and at this moisture content the glass transition temperature of hemicellulose and lignin is about 200˚C. Hence by cooling the platens to 120˚C the strategy of VTC processing was not violated as the temperature was still below the glass transition temperature of the individual components of wood when the compression force was released.

Visual observation revealed that the phenol-formaldehyde resin used to make the strand composite performed well in the atmosphere of 170˚C and 862 KPa (125 psi) steam pressure. There was no obvious deterioration observed in the VTC processed samples and

the adhesion of the strands remained intact. Also there were pockets of dark coloration observed on the surface of the processed samples. This might be due to the accumulation of the volatile components present in the wood.

It is recommended that the VTC device be refined to obtain better control and performance. If the device had a dedicated hydraulic system, to provide the required compression force, then it would greatly enhance the efficiency of the system and make it more user friendly. This could happen if the device is provided with an independent hot press for its operation. In this case it would be advisable to have the lid of the device attached to the top platen of the hot press as this would make the process of loading and unloading specimens faster. Also, the nut and bolt system to secure the lid to the chamber is very laborious at high temperatures. A quick clamp system would contribute to lowering the time required to process a sample and help to maintain a constant temperature.

Thermal insulation has been an issue while making the test specimens. Temporary solutions have been provided, but permanent solutions are needed. There are two places where insulation would improve the performance. Firstly, heat transfer should be restricted from the lid to the top platen. This would help control the specimen temperature accurately and result in consistent exposure of the specimens to a particular temperature. Currently a ceramic-based, half-inch thick sheet has been installed to insulate the top and bottom platens (Zircar Refractory Composites, Inc., Florida, New

York, product #RSLE-57). Thicker insulation is needed. However, the chamber has an interior height limitation. Perhaps the metal platen could be reduced in thickness to accommodate additional insulation. The insulation must possess adequate compression strength and survive the steam environment as well. Secondly, the stainless steel bellows has high surface area and loses heat quite rapidly. This condenses the steam inside the unit very quickly and requires more time to reach the target pressure. A temporary solution included a thin sheet of fibrous blanket insulation (approximately 25 mm (1-inch) thick uncompressed). As a result the symptoms of condensation were reduced. However, this insulation wears out as a result of rough handling during removal and insertion of the device in the hot press. This problem would be solved if a dedicated hot pressed were used.

5.2 Enhancement of the flexural properties of the oriented strand composite using high density VTC strands:

The final mechanical property of the wood composite panel is strongly defined by the final panel density. This would mean that a high compaction ratio for making a composite would result in superior mechanical properties of the final product (Hsu 1997). However, there has been evidence that even minor deviation from parallel strand alignment can drastically alter the flexural properties of the panel and hence density cannot be the only deciding factor (Nishimura and Ansell 2002). Also, higher density of the surfaces compared to the core occurs normally in hot-pressing of strand composites.

This is advantageous and results in a higher bending strength. In this treatment we attempted to enhance surface density by incorporating higher density VTC strands in the surface without increasing the overall density of the panel.

Conventional VTC processing involves annealing of the sample to 200˚C after the second stage compression. This step is intended to decrease the hygroscopicity of the wood by partially decomposing the hemicelluloses in the wood substance. This step was not performed while making the VTC strands due to the lack of heated platens for multiple platen design inside the small VTC device. The multiple platen arrangement was needed to increase the processing capacity and meet the requirements of the project in the given time frame. Around 2,500 strands were required to make the test panels and one VTC process required about 20 minutes. Hence it was decided to make 18 strands per batch in the multi-platen arrangement. Also, the target strand density to be achieved was set over $1g/cm^3$, but the average VTC strand density attained was about $0.91g/cm^3$. This may be due to the unexpected amount of springback due to the lack of the annealing step. The lack of an annealing step may also help to explain that the thickness swell with the inclusion of 20% and 40% by weight of VTC strands was higher than their respective controls.

The treatment with 20% VTC strands on the surface didn’t quite yield the expected result. This might be due to the lack of continuity of the high density strands on the surface. Since the VTC strands were about 2.5 times higher in density than non-VTC

strands, there were about 2.5 times fewer VTC strands to orient in the surface layer. The failure in the bending specimens was usually observed in the gaps between the VTC strands on the surface. On the other hand, a continuous surface of high density strands was obtained with the addition of 40% by weight of VTC strands. Perhaps this explains the statistical significance in MOE with the inclusion of 40% VTC strands.

The resin used in this study was commercially available phenol-formaldehyde OSB face resin. There was no attempt to optimize resin performance in regard to bonding VTC strands. Furthermore, all strands were blended together and then separated prior to mat formation. Most of the failures observed in the samples after testing were at the interface between the VTC strands and the normal strands. This was very evident with the internal bond samples. It was possible that the VTC strands, being the high density strands, have lower penetration of the resin compared to the lower density normal strands, resulting in weaker bond strength. Kutnar et al. (2008) studied the bond performance of laminated VTC composites from hybrid poplar using PF resin. They reported resin penetration into VTC wood (densified 63 to 132%) was about 50 to 70% less than normal hybrid poplar. Simple 3-layer composites were tested in bending, with outer layers made of VTC wood and the center layer from normal wood. Whereas some specimens failed in shear at the bondline, most failed in the tensile-side VTC layer, which indicated that bonding VTC wood to normal wood was not particularly problematic. Atomized PF resin on the surface of wood strands, however, may behave different than a continuous bondline. The question of bond performance of VTC wood strands deserves further study.

If the study is performed again then the following suggestions may prove to be effective. Firstly, resin optimization testing should be performed to improve bonding of VTC strands to normal strands and to each other. This would minimize doubts, if any, concerning possible shear-slip between the VTC and the normal strands. Secondly, VTC strands should be produced that have higher specific gravity than 0.9 g/cm^3. This can be achieved in two ways. If the strands prior to densification have greater thickness, then the VTC processing would produce higher density strands using the same procedure described in this report. An alternative could be incorporating the annealing step, which was omitted from this research. Heat treatment would decrease the amount of springback in the strands after densification. This in turn would reduce the number of strands, due to the greater mass per strand, to cover the OSC surface and result in a tradeoff. A continuous surface of VTC material could also be achieved by using a sheet of veneer which has been densified by the VTC process. This would provide complete coverage with minimum possible weak links (knots). If VTC veneer is ever used, then the hot press operation should be modified accordingly. This is because the high density sheet of veneer would reduce mass transfer from the surface and increase the internal mat steam pressure. Perhaps a longer venting time, reduced mat moisture content, or intermediate vent step could be modifications used to accommodate a sheet of VTC veneer. Thirdly, there is a threshold percentage (which lies between 20% and 40%) of VTC strands above which the flexural properties increase dramatically. This number is quite critical and very important to be known.

5.3 Strand Composite modified by the VTC process.

The primary intent of the strand composite modified by the VTC process is not to be used as a stand-alone product, but as surface layers in a multi-layered composite material. Based on the premise of the classical lamination theory, the non-VTC lamina configured with the VTC lamina on either side enhanced the bending properties. The bending performance of the three-layered composite was also dependent on the lamina to lamina adhesion.

Preliminary tests to determine the hot press schedule and best resin application procedure were conducted using 4-inch square samples and a small laboratory press (15 cm by 15 cm (6-inch by 6-inch) platens). The schedule selected specified the 3-layer composite to be pressed at 1034 KPa (150 psi) at 180˚C. However, when these press conditions were tried upon the 41 cm by 23 cm (16-inch by 9-inch) samples, it resulted in a blow (delamination due to steam pressure). Visual observation of the sample after it was cut open revealed that the VTC laminates and the bondlines were intact. The brunt of the damage was held within the core layer of the normal strand composite, where a large void developed in the center of the panel. The cause of the blow was identified as inadequate venting of internal steam pressure as a result of low permeability of the VTC lamina. To reduce the chance of a blow among the remaining specimens, two adjustments to the press schedule were adopted. It was decided to reduce the temperature of the press platens to 150˚C. Since the VTC laminas were high density, they also had a greater

thermal conductivity than a normal strand composite. Therefore, the bondline temperature could easily achieve 120^{o}C with only 150^{o}C platen temperature. The saturated steam pressure at 180˚C is approximately 1000 KPa (145 psi). The saturated steam pressure at 150˚C is approximately 476 KPa (69 psi). The 30˚C reduction in platen temperature dropped the potential internal steam pressure by half and significantly reduced the chance of a blow. Also, the reduction in compressive force by one third after the first 5 minutes of pressing helped ease the developing steam pressure inside the mat.

It was stated in the results that there was no significant statistical difference between the three different levels of densification. The actual densities obtained from the treatment were then compared to the target densities. This revealed that the samples with 122% and 71% target degree of densification were off by a factor of 12% and 42%. It is well known that all strand composites have a horizontal density distribution. Localized density measurements in the panels were performed. The panels were cut into 50 mm (2-inch) squares and the density determined for each piece. The horizontal density distribution plots are shown in Figure 5.3.1, Figure 5.3.2 and Figure 5.3.3. This illustrated that there were high density pockets in the panel, that when compressed in the VTC apparatus, achieved their maximum density of 1.4 g/cm^3 (87 pcf) before the average panel density reached the target value. Previous experience with VTC wood has shown that a specific gravity of about 1.4 is the maximum obtainable since this approached the specific gravity of the cell wall substance. This explains the unexpected behavior of the higher target density treatment. With the 94% and 71% target degree of densification, there was no

statistically significant difference observed in the actual density levels. The mean density values were found to be 1.1 g/cm^3 (67 pcf) and 1.01 g/cm^3 (62 pcf), which correspond to an increase of 86% and 72%, respectively. These values were close to the target densities, but the variability was too high to declare a statistically significant difference. Therefore, the only main affect that this study revealed was the difference in density and MOE before and after VTC processing.

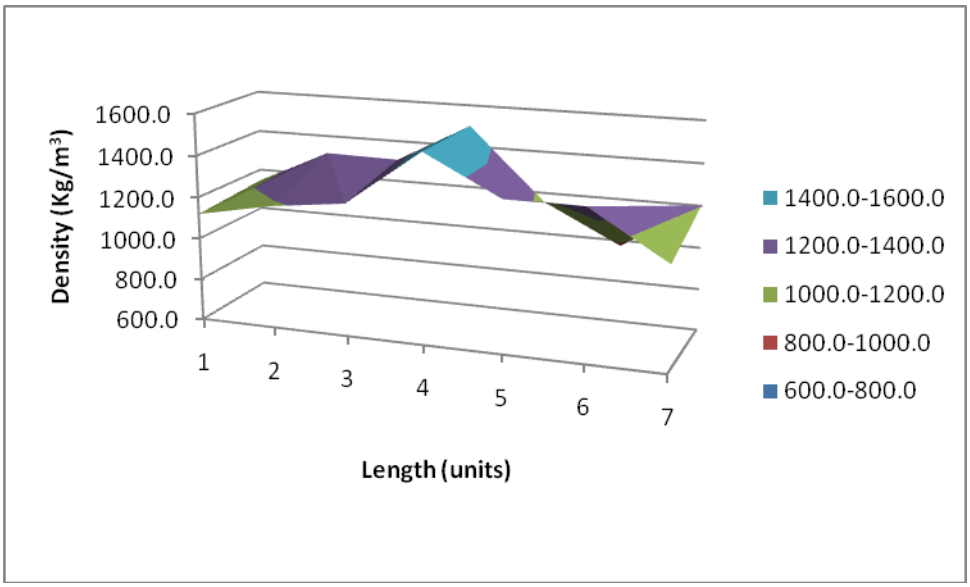

Figure 5.3.1: Horizontal density distribution for 122% densification level.

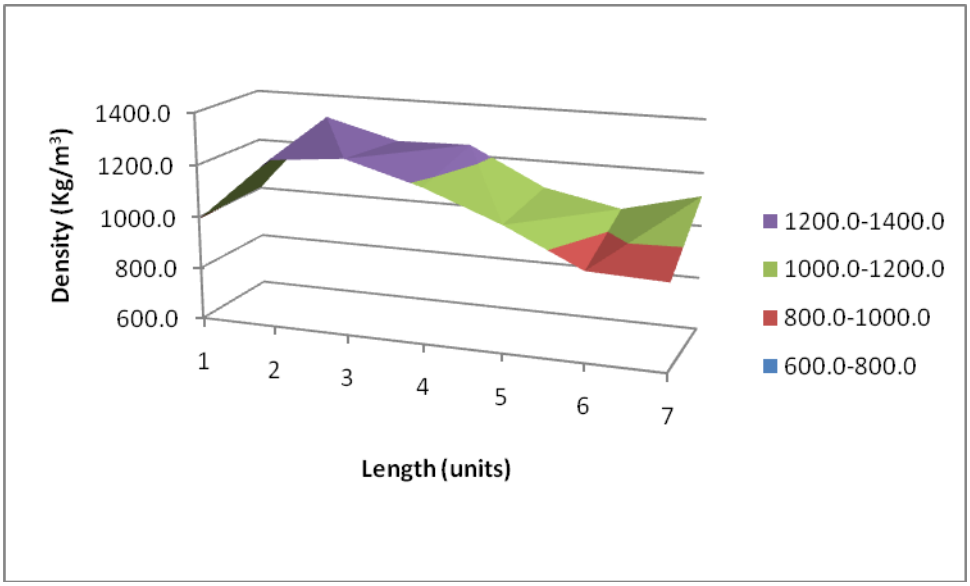

Figure 5.3.1: Horizontal density distribution for 94% densification level

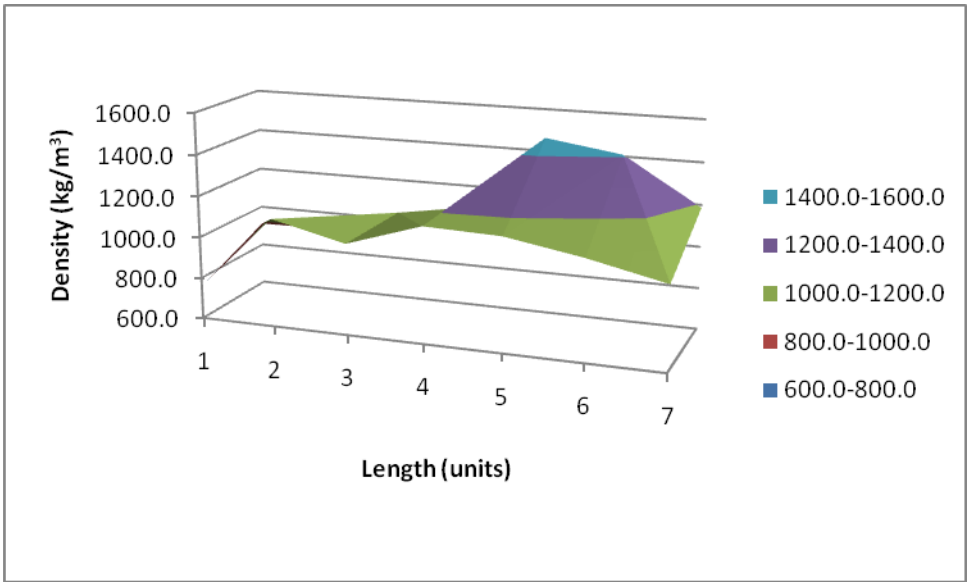

Figure 5.3.1: Horizontal density distribution for 71% densification level

Chapter 6: Conclusions

Bending properties of the wood strand composites manufactured in this study were successfully increased using the VTC process. These results were observed in the low density, diffuse porous, hardwood species hybrid poplar. Three main objectives of the study were met. Firstly, the scale-up device was successfully constructed and operated to produce VTC specimens. The intent of the construction was to process samples of larger dimension (61 cm by 25 cm), which was accomplished. The major difference associated with the process procedure of the scale-up device was that the platens in the cooling stage were brought down to 120 ˚C instead of cooling them below 100 ˚C as was done in the smaller VTC device.

Secondly, bending properties of the oriented strand composite was improved with the inclusion of high density VTC strands. The MOE of the VTC strands increased by 100% and the observed increase in density was found to be 133%. There was a dramatic increase in the MOE values among the oriented strand composite with the simple process of orientation. Panels with 20% and 40% by weight of normal strands (no VTC strands) oriented on the surface showed a dramatic increase in the MOE, by 55% and 64%, and MOR, by 22% and 33%, respectively. With the inclusion of 20% VTC strands, which were oriented on the surface, there was no statistically significant increase of MOE and MOR. The addition of 40% VTC strands improved the MOE and MOR by 30% and 18%, respectively. It is proposed that a continuous layer of strands was achieved with 40%

inclusion of VTC strands and hence the dramatic rise in the flexural properties. Furthermore, qualitative observation among the bending test samples revealed that the failure mostly occurred either between the interface of normal and VTC strands or in the non-continuous layer. Of particular note, the enhancement of bending properties was achieved without increasing the overall panel density.

Lastly, the properties of the VTC processed strand board were evaluated. Three target densification levels were attempted. However, local variation in panel density (high density pockets) likely prohibited VTC strand board density above an average of about 1089 Kg/m^3 (67 pcf). Nevertheless, VTC processing of strand board yielded MOE increase of 152% to 162%. When bonded into a three-layered composite, with a non-VTC core, the MOE was increased by 57 to 80% in comparison to the strand board prior to VTC processing.

Reference

Back, E.L., N.L. Salmen. 1982. Glass transitions of wood components hold implications for molding and pulping processes. Tappi Journal, 65(7): 107-110.

Barnes, D. 2001. A model of the effect of strand length and strand thickness on the strength properties of oriented wood composites. Forest Products Journal. 51(2):36-46.

Bodig, J. and B. A. Jayne. 1982. Mechanics of wood and wood composites. Van Nostrand Reinhold Company, New York, NY.

Bryane. L. 1962. Dimensional stability of particleboard. Forest Prod. J. 12(12):572 - 576.

Casey, L.J. 1987. Changes in wood-flake properties in relation to heat, moisture, and pressure during flakeboard manufacture. MS Thesis, VPI & SU, 162p.

Chawla, J.S. and A.N. Sharma, 1972. Experiments on tempering of fibreboards. In. Acad. Wood Sci. 2:70-73.

Clark, Judy, 2001. The global wood market, prices and plantation investment: an examination drawing on the Australian experience. Foundation for Environmental Conservation. Environmental Conservation 28 (1): pp. 53–64.

Cowie, J.M.G. 1991. Polymers: chemistry and physics of modern materials. Blackie Academical & Professional, Glasgow.

Dwianto, W., Inoue, M., Norimoto, M.,1998. Permanent fixation of compressive deformation Albizia wood. (*Paraserienthes falcate*) by heat treatment. Journal of Tropical Forest Products, 4(1). p. 59 – 67.

Erickson, E.C.O. 1965. Mechanical properties laminated modified wood. No. 1039, Forest products laboratory. 39pp.

FPL-GTR-149, 2003. Fundamentals of composite processing. Proceedings of a workshop.

Garcia, P.J., Avramidis, S., Lam, F. 2003. Horizontal gas pressure and temperature distribution responses to OSB flake alignment during hot-pressing. Holz als Roh- und Werkstoff 61:425–431.

Gardner, D.J., D.W. Gunnells, M.P. Wolcott, L.Amos.1993. Changes in wood polymers during the pressing of wood composites. Cellulosics: Chemical, Biochemical and Material Aspects, p. 513-518.

Geimer, Robert L., Kwon, Jin Heon., 1999. Flakeboard thickness swelling . Part II. Fundamental response of board properties to steam injection pressing. Wood and Fiber Science. 31(1): 15-27

Geimer, R. L., R.J. Mahoney, S.P. Loehnertz, and R. W. Meyer. 1985. Influence of processing induced damage on strength of flakes and flakeboards. USDA-FS Forest Products Laboratory Research Paper FPL 463.

George Tsuomis 1991. Science and Technology of Wood. Pp.111-213

Gerhards, C.C. (1982). Effect of moisture and temperature on the mechanical properties of wood: An analysis of immediate effects. *Wood Fiber* 14(1):4–36.

Giebeler, E., Dimensional stabilization of wood by moisture-heat-pressure. Holz Roh-Werkst. 41:87-94 (1983).

Goring D.A.I. 1963. Thermal softening of lignin, hemicellulose and cellulose. Pulp and Paper Magazine of Canada, pp 517–527.

Heger, F., Groux, M., Girardet, F., Welzbacher, C., Rapp, A. O., Navi, P., 2004. Mechanical and durability performance of THM-densified wood. In: proc. Environmental Optimization of Wood Protection Workshop, Lisboa – Portugal, 22nd-23rd March 2004.

Hillis, W.E., A.N. Rozsa. 1978. The softening temperatures of wood. Holzforschung, 32, H.2: 68-73.

Hillis W, 1984. High temperature and chemical effects on wood stability. I. General considerations. Wood science and technology. 18(4):281-293.

Hoadley, R. B., 2000. Understanding Wood; A Craftsman's Guide to Wood Technology. Taunton Press, Newton, Connecticut. Ch. 4, p. 75 – 101.

Hoover WL, Hunt MO, Lattanzi RC, Bateman JH, Youngquist JA (1992) Modelling mechanical properties of single-layer, aligned, mixed-hardwood strand panels. For Prod J 42:12–18.

Hsu, W. E. 1987. A process for stabilizing waferboard and OSB. Pages 219-236 in Proc. 21th Washington State University International Symposium on Particleboard. Pullman, WA.

Hsu, W.E., W. Schwald, J. Schwald, J.A. Shields 1988. Chemical and physical changes required for producing dimensionally stable wood-based composites. Part I: Steam pretreatment. Wood Science and Technology, 22: 281-289.

Hsu, W.E. 1997. Wood quality requirements for panel products. In Proceedings of CTIA/IUFRO International Wood Quality Workshop, Timber Management Toward Wood Quality and Endproduct Value, 18–22 August 1997. Edited by S.Y. Zhang, R. Gosselin, and G. Chauret. Forintek Canada Corp., Sainte-Foy, Que. I-7/10.

Hunt MO, Suddarth SK (1974) Prediction of elastic constants of particleboard. For Prod J 24:52–57.

Inoue, M., M. Norimoto, M. Tanahashi, R.M. Rowell 1993. Steam or heat fixation of compressed wood. Wood and Fiber Science, 25(3): 224-235.

Inoue, M., N. Sekino, T. Morooka, M. Norimoto. 1996. Dimensional stabilization of wood composites by steaming I. Fixation of compressed wood by pre-steaming. *In* Proceedings from the Third Pacific Rim Bio-Based Composites Symposium, Kyoto, Japan. pp. 240-248.

Irvine G (1984). The glass transitions of lignin and hemicellulose and their measurement by differential thermal analysis. Tappi J 67(5):116–121.

Kamke, F. A. and L. J. Casey. 1988a. Gas pressure and temperature in the mat during flakeboard manufacture. Forest Products Journal, 38(3):41-43.

Kamke, F.A., L.J. Casey 1988b. Fundamentals of flakeboard manufacture: internal-mat conditions. Forest Products Journal, 38(6): 38-44.

Kamke, F.A.,E.V. Kultikova, and C.A. Lenth. 2000. Viscoelastic thermal compression of wood. Proc., 5th Pacific-Rim Bio-Based Composites Symp. Dec. 10-13.2000, Canberra, Australia, p.292-302.

Kawai, S., Q. Wang, H. Sasaki, M. Tanahashi. 1992. Production of compressed laminated veneer lumber by steam pressing. In Proceedings of the Pacific Rim Bio-Based Composites Symposium, p. 121-128.

Kelley, S.S., T.G. Rials, W.G. Glasser 1987. Relaxation behavior of the amorphous components of wood. Journal of Materials Science, 22: 617-624.

Kollmann, F. P., E.W. Kuenzi, A.J. Stamm. 1975. Principles of wood science and technology. Vol. II Wood based materials. Springer-Verlag New York Heidelberg Berlin. pp. 139-149.

Kollmann, F., and Cote, W.A., Jr. (1968). *Principles of Wood Science and Technology*. Vol. 1. Solid Wood; Springer-Verlag, Berlin.

Kutnar, A.; F.A. Kamke and M. Sernek. 2008. The mechanical properties of densified VTC wood relevant for structural composites. Holz als Roh- Werkst. 66(6): 439-446

Laufenberg, T. L. 1984. Flake board fracture surface observations and correlation with orthotropic failure criteria. Journal of Institute of Wood Science. 10(2):57-65.

Lawther J, Sun R, Banks W. Rapid isolation and structural characterization of alkali-soluble lignins during alkaline treatment and atmospheric refining of wheat straw. Industrial crops and products. June 1996; 5(2):97-105

Lenth, C.A. and F.A. Kamke. 2001b. Moisture dependent softening behavior of wood. Wood and Fiber Sci. 33(3):492-507.

LeVan, S.M., Ross, R.J., and Winandy, J.E. (1990). Effects of fire retardant chemicals on the bending properties of wood at elevated temperatures. USDA Research Paper FPL-RP-498, Madison, WI.

Li, M.; M. P. Wolcott, F. A. Kamke, and D. A. Dillard. 1990. Small specimen compression testing in a pressurized steam environment. Exper. Tech. May/June, p. 17-19.

Liu, J. Y., and J. D. McNatt. 1991. Thickness swelling and density variation in aspen flakeboards. Wood Sci. Technol. 25(1):73-82.

Miyamoto, Kohta. Shigehiko Suzuki. Takayoshi lnagaki. Ritsuo Iwata Effects of press closing time on mat consolidation behavior during hot pressing and on linear expansion of particleboard. J Wood Sci (2002) 48:309-314

N. L. Salmen and E. L. Black, TAPPI 60(12) (1977) 137. W. J. Cousins, Wood Science Technology. 10 (1976) 9.

Navi, P., Giradet, F., 2000. Effects of thero-hygro-mechanical treatment on the structure and properties of wood. Holzforschung (54). p. 287 – 293.

Nishimura, T., Ansell, M.P. (2002) Monitoring fiber orientation in OSB during production using filtered image analysis. Wood Sci. Technol. 33:85–95.

O'Conner J.P. (2007) Improving wood strength and stiffness through viscoelastic thermal compression. MS thesis, Oregon State University, Corvallis, OR. Pp. 56-68.

Price, E.W. 1976. Determining tensile properties of sweetgum veneer flakes. Forest Prod. J. 26(10):50-53.

Rowell, M. Roger. 2005. Wood chemistry and wood composites. pp 10-32.

Rowell, R. M and R. L. Youngs. 1981, Dimensional stabilization of wood in use. U.S Forest Production Laboratory. FPL – 0243.

Rowell, R., Lange, S., McSweeny, J., Davis, M., 2002. Modification of wood fiber using steam. In: proc. The 6th Pacific Rim Bio-based Composites Symposium. p. 606 – 615.

Rowell, R.M. (1980). *How the Environment Affects Lumbar Design*, Lyon, D.E. and Galligan, W.L. (Eds.), USDA, Forest Service, Forest Products Laboratory Report.

Rowell, R.M., P. Konkol. 1987. Treatments that enhance physical properties of wood. FPL, General Technical Report FPL-GTR-55, 12 pp.

Salmen, L., and E. L. Back. 1977. The influence of water on the glass transition of cellulose. *Tappi* 60(12):137-140.

Seborg, R.M., H. Tarkow, A.J. Stamm. 1962. Modified woods. FPL, Report No. 2192(revised), 30 pp.

Seborg, R.M., M.A. Millett, A.J. Stamm. 1962. Heat-stabilized compressed wood (Staypak). FPL, Report No. 1580 (revised), 22 pp.

Semple, Kate E., Marie-Helene Vaillant, Kyu-Young Kang, Seung Won Oh, Gregory D. Smith and Shawn D. Mansfield. 2007. Evaluating the suitability of hybrid poplar clones for the manufacture of oriented strand boards. Holzforschung, Vol. 61, pp. 430–438.

Skaar, C. Effect of high temperature on the rate of degradation and reduction in hygroscopicity of wood. Proceedings, High temperature drying effects on mechanical properties of softwood lumber, C.C. Gerhards and J.M. McMillen (eds), February 25-26, 113-127, USDA, Forest Service, Forest Products Laboratory, Madison, WI (1976).

Stamm, A. J., Wood and Cellulose Science; The Ronald Press Co., New York, NY (1964).

Stamm, A.J. and L.A. Hansen, Minimizing wood shrinkage and swelling: Effects of heating in various gases, Ind. Eng. Chem. 29(7):831-833 (1937).

Stamm, A.J., R. M. Seborg. 1941. Resin treated, laminated, compressed wood. Trans. Am. Inst. Chem. Eng., 37:385-397.

Steiner and C. Dai. 1993. Spatial structure of wood composites in relation to processing and performance characteristics: Part I. Rationale for model development. Wood Sci. Technol. 28:45-51.

Structural board association, 2000. Performance by design – Oriented Strand Board (OSB).

Sun, B. C. H., R. N. Hawke, and M. R. Gale. 1994a. Effect of polyisocyanate level on physical properties of wood fiber composite materials. Forest Products Journal. 44(3):34-40.

Sun, B. C. H., R. N. Hawke, and M. R. Gale. 1994b. Effect of polyisocyanate level on physical properties of wood fiber composite materials. Forest Products Journal. 44(4):53-58.

Suo and Bowyer, 1995. Modelling of strength properties of structural particleboard. Wood Fiber Science, 21(1). pp. 84-94.

Tiemann H. D. 1906. Effect of moisture upon the strength and stiffness of wood. U. S. Dep. Agric. For. Serv. Bull. 70. 144pp.

Tomme, P., Girardet, F., Gteller, B., Navi, P., 1998. Densified wood: An innovative product with highly advanced characters. In: proc. World Conference on Timber Engineering Montreux-Lansanne, Switzerland August 17th -20th 1998.

USDA, 1999. Wood Handbook: Wood as an engineering material. Copyright USDA Forest Service Forest Products Laboratory. Ch. 3 – 4.

Viitaniemi, P. and S. Jamsa, Modification of wood with heat treatment. VTT Julkaisuja, Publication number 814, Espoo, Finland (1996).

Wilson, J. B. 1982. Durability as affected by resin type. General Technical Report SO-53. USDA Forest Service. Southern Forest Experiment Station. 53-57.

Wilson, T.R.C. (1932). Strength-moisture relations for wood. USDA Tech. Bull. No. 282, Washington, DC.

Winistorfer, Paul M. William W. Moschler, Jr. Siqun Wang, Esteavo DePaula, Bobby L. Bledsoe, 2000. Fundamentals of vertical density profile formation in wood composites. Part – I. insitu density measurement of the consolidation process. Wood and Fiber Science. 32(2), pp 209-219

Wolcott, M. P.; B. Kasal; F. A. Kamke and D. A. Dillard. 1989. Testing small wood specimens in transverse compression. Wood and Fiber Sci., 21(3):320-329.

Wolcott, M. P.; F. A. Kamke, and D. A. Dillard. 1994. Fundamental aspects of wood deformation pertaining to manufacture of wood-based composites, Wood and Fiber Sci. 26(4):496-511.

Wolcott, M. P.; F. A. Kamke, and D. A. Dillard. 1994. Fundamental aspects of wood deformation pertaining to manufacture of wood-based composites, Wood and Fiber Sci. 26(4):496-511.

Wolcott, M.P., F.A. Kamke, D.A. Dillard. 1990. Fundamentals of flakeboard manufacture: viscoelastic behavior of the wood component. Wood and Fiber Science, 22(4): 345-361.

Wu and Suchsland, 1997. Effect of moisture on the flexural properties of commercial oriented strandboards. Wood Fiber Sci. 29(1):47-57.

Wu, Q. and C. Piao. 1999. Thickness swelling and its relationship to internal bond strength loss of commercial oriented strandboard. Forest Products Journal. 49(7/8):50-55.

Wu, Q. and O. Suchsland. 1997. Effect of moisture on the flexural properties of commercial oriented strandboard. Wood and Fiber Science. 29(1):47-57.

Appendices:

Appendix A: Raw data for VTC strands and OSC modified by inclusion VTC strands.

Table A1: Hybrid Poplar weight and volume raw data before and immediately after VTC processing. Wet strands were stored in cold room at -10˚C until VTC processing.

	Before Compression					After Compression		
	Wt	Volume	Wet Density	Est. MC	Est. OD Density	Wt (a)	Volume	Density
Sample Number	g	cm3	g/cm3	%	g/cm3	g	cm3	g/cm3
1	4.44	7.31	0.607	76.9	0.34	2.51	3.70	0.68
2	5.08	7.45	0.682	77.0	0.39	2.87	3.93	0.73
3	5.38	8.07	0.666	50.7	0.44	3.57	4.00	0.89
4	5.68	7.38	0.769	56.5	0.49	3.63	3.72	0.98
5	6.4	7.98	0.802	70.2	0.47	3.76	3.94	0.95
6	3.25	4.40	0.738	79.6	0.41	1.81	2.84	0.64
7	6.26	7.50	0.835	93.8	0.43	3.23	3.64	0.89
8	5.48	7.32	0.749	83.9	0.41	2.98	3.37	0.88
9	6.01	7.48	0.803	72.7	0.47	3.48	3.73	0.93
10	3.62	7.29	0.497	58.8	0.31	2.28	2.84	0.80
11	6.03	7.07	0.853	131.9	0.37	2.6	2.91	0.89
12	5.1	6.41	0.795	66.7	0.48	3.06	3.72	0.82
13	4.72	7.30	0.647	61.6	0.40	2.92	3.84	0.76
14	4.74	7.22	0.656	59.6	0.41	2.97	3.52	0.84
15	6.09	8.10	0.752	95.8	0.38	3.11	3.35	0.93
16	4.09	6.29	0.650	69.0	0.38	2.42	3.04	0.80
17	3.98	7.19	0.554	50.2	0.37	2.65	3.52	0.75
18	6.17	8.45	0.730	142.9	0.30	2.54	3.82	0.67
19	5.1	7.86	0.649	64.5	0.39	3.1	3.80	0.82
20	5.03	8.19	0.614	67.1	0.37	3.01	4.14	0.73
21	5.08	8.79	0.578	78.9	0.32	2.84	3.62	0.78
22	4.84	8.05	0.601	64.6	0.37	2.94	3.42	0.86
23	5.12	7.65	0.669	76.6	0.38	2.9	3.76	0.77
24	5.09	7.57	0.673	64.2	0.41	3.1	4.13	0.75
25	5.04	7.45	0.676	66.3	0.41	3.03	3.52	0.86
26	5.21	7.66	0.680	70.3	0.40	3.06	4.13	0.74
27	5.36	8.15	0.658	53.6	0.43	3.49	4.23	0.83
28	3.86	5.65	0.684	77.1	0.39	2.18	3.25	0.67
29	5.35	8.30	0.645	82.6	0.35	2.93	3.59	0.82
30	4.94	7.27	0.679	58.8	0.43	3.11	3.59	0.87
31	6.04	8.05	0.751	74.1	0.43	3.47	3.23	1.07

	Before Compression					After Compression		
	Wt	Volume	Wet Density	Est. MC	Est. OD Density	Wt (a)	Volume	Density
Sample Number	g	cm3	g/cm3	%	g/cm3	g	cm3	g/cm3
32	5.95	7.49	0.795	115.6	0.37	2.76	2.93	0.94
33	6.3	7.61	0.828	109.3	0.40	3.01	3.14	0.96
34	4.7	7.75	0.606	67.9	0.36	2.8	3.51	0.80
35	4.02	7.45	0.539	13.6	0.47	3.54	3.51	1.01
36	4.98	7.59	0.656	90.1	0.35	2.62	2.92	0.90
37	4.92	7.63	0.645	95.2	0.33	2.52	2.83	0.89
38	4.96	7.98	0.622	71.6	0.36	2.89	2.63	1.10
39	5	7.59	0.658	68.4	0.39	2.97	3.27	0.91
40	4.5	7.14	0.630	53.1	0.41	2.94	3.04	0.97
41	4.72	6.44	0.732	66.2	0.44	2.84	2.72	1.05
42	4.18	6.88	0.608	53.7	0.40	2.72	2.97	0.91
43	4.09	7.14	0.572	51.5	0.38	2.7	3.06	0.88
44	4.21	7.04	0.598	43.2	0.42	2.94	2.81	1.05
45	3.82	6.77	0.564	67.5	0.34	2.28	2.65	0.86
46	4.43	7.06	0.628	51.2	0.42	2.93	2.71	1.08
47	5.14	7.13	0.721	104.0	0.35	2.52	2.23	1.13
48	4.93	6.51	0.757	70.0	0.45	2.9	2.97	0.98
49	4.54	7.41	0.612	61.6	0.38	2.81	3.02	0.93
50	5.93	7.76	0.764	68.9	0.45	3.51	3.08	1.14
51	4.02	7.21	0.558	50.0	0.37	2.68	2.86	0.94
52	3.28	6.68	0.491	29.6	0.38	2.53	2.62	0.97
53	3.73	7.84	0.476	25.6	0.38	2.97	2.91	1.02
54	3.48	7.34	0.474	21.3	0.39	2.87	2.90	0.99
55	4.86	7.51	0.647	59.9	0.40	3.04	3.60	0.84
56	3.32	7.22	0.460	26.2	0.36	2.63	2.61	1.01
57	4.48	7.61	0.589	66.5	0.35	2.69	3.01	0.89
58	4.48	7.84	0.572	50.8	0.38	2.97	3.26	0.91
59	5.25	7.18	0.731	83.6	0.40	2.86	2.60	1.10
60	4.16	7.76	0.536	71.2	0.31	2.43	2.93	0.83
61	3.94	7.64	0.516	44.9	0.36	2.72	2.87	0.95
62	4.34	6.86	0.633	50.7	0.42	2.88	2.74	1.05
63	3.85	6.61	0.583	69.6	0.34	2.27	2.55	0.89
64	4.94	6.98	0.708	80.3	0.39	2.74	2.74	1.00
65	5.33	7.78	0.685	73.1	0.40	3.08	3.16	0.97
66	6.19	7.69	0.805	101.6	0.40	3.07	3.18	0.96
67	3.32	7.88	0.421	23.9	0.34	2.68	2.87	0.93
68	7.7	7.39	1.041	236.2	0.31	2.29	2.36	0.97
69	6.65	8.44	0.788	133.3	0.34	2.85	2.91	0.98
70	3.33	6.78	0.491	27.1	0.39	2.62	2.89	0.91
71	3.69	7.84	0.471	37.7	0.34	2.68	2.84	0.94
72	7.55	7.88	0.958	226.8	0.29	2.31	2.66	0.87

	Before Compression					After Compression		
	Wt	Volume	Wet Density	Est. MC	Est. OD Density	Wt (a)	Volume	Density
Sample Number	g	cm3	g/cm3	%	g/cm3	g	cm3	g/cm3
73	6.15	7.73	0.796	119.6	0.36	2.8	3.19	0.88
74	5.61	7.06	0.794	108.6	0.38	2.69	2.92	0.92
75	5.82	7.52	0.774	83.0	0.42	3.18	3.38	0.94
76	6.61	8.40	0.787	118.2	0.36	3.03	3.63	0.84
77	5.09	6.76	0.753	96.5	0.38	2.59	2.99	0.87
78	4.97	7.53	0.660	64.0	0.40	3.03	3.71	0.82
79	4.28	8.03	0.533	65.3	0.32	2.59	3.11	0.83
80	5.39	6.92	0.779	94.6	0.40	2.77	2.77	1.00
81	3.6	6.78	0.531	51.3	0.35	2.38	2.75	0.86
82	4.1	7.67	0.535	49.1	0.36	2.75	3.19	0.86
83	6.88	7.00	0.982	229.2	0.30	2.09	2.42	0.86
84	4.65	7.30	0.637	71.0	0.37	2.72	3.13	0.87
85	6.06	6.87	0.883	114.9	0.41	2.82	3.03	0.93
86	4.5	7.49	0.601	73.7	0.35	2.59	3.03	0.85
87	4.63	7.96	0.581	65.9	0.35	2.79	3.12	0.89
88	3.54	7.45	0.475	36.7	0.35	2.59	2.59	1.00
89	7.16	7.60	0.942	121.0	0.43	3.24	3.97	0.82
90	4.28	7.26	0.589	71.9	0.34	2.49	2.70	0.92
91	4.03	6.72	0.599	68.6	0.36	2.39	2.77	0.86
92	4.24	7.42	0.572	69.6	0.34	2.5	2.72	0.92
93	5.45	6.66	0.818	91.2	0.43	2.85	2.61	1.09
94	3.05	4.44	0.687	54.0	0.45	1.98	2.30	0.86
95	4.82	6.52	0.739	82.6	0.40	2.64	2.69	0.98
96	5.28	6.93	0.762	95.6	0.39	2.7	3.10	0.87
97	5.78	6.53	0.886	152.4	0.35	2.29	2.41	0.95
98	3.31	6.19	0.535	63.1	0.33	2.03	2.42	0.84
99	5.37	6.77	0.793	92.5	0.41	2.79	2.96	0.94
100	5.22	7.29	0.716	81.3	0.39	2.88	3.17	0.91
101	3.75	6.34	0.592	62.3	0.36	2.31	2.53	0.91
102	4.06	6.36	0.639	91.5	0.33	2.12	2.28	0.93
103	4.44	7.04	0.630	70.8	0.37	2.6	2.94	0.89
104	5.18	7.43	0.697	82.4	0.38	2.84	2.88	0.99
105	3.75	6.94	0.540	52.4	0.35	2.46	2.93	0.84
106	4.98	7.25	0.687	76.0	0.39	2.83	2.86	0.99
107	5.96	8.29	0.719	86.8	0.38	3.19	3.43	0.93
108	4.41	7.11	0.620	61.5	0.38	2.73	2.52	1.08
109	4.38	6.73	0.651	81.7	0.36	2.41	2.65	0.91
110	6.66	7.11	0.937	125.0	0.42	2.96	2.75	1.08
111	3.98	8.00	0.498	47.4	0.34	2.7	3.00	0.90
112	4.07	6.96	0.585	75.4	0.33	2.32	2.64	0.88
113	6.56	8.12	0.808	103.1	0.40	3.23	3.62	0.89

	Before Compression					After Compression		
	Wt	Volume	Wet Density	Est. MC	Est. OD Density	Wt (a)	Volume	Density
Sample Number	g	cm3	g/cm3	%	g/cm3	g	cm3	g/cm3
114	4.89	8.03	0.609	74.0	0.35	2.81	3.14	0.89
115	5.88	8.19	0.718	82.0	0.39	3.23	3.08	1.05
116	4.3	8.39	0.513	56.9	0.33	2.74	3.02	0.91
117	4.83	7.80	0.619	74.4	0.35	2.77	2.77	1.00
118	3.38	6.51	0.520	23.8	0.42	2.73	2.65	1.03
119	4.69	8.56	0.548	62.8	0.34	2.88	2.81	1.02
120	3.48	7.67	0.454	37.5	0.33	2.53	2.98	0.85
121	5.69	8.59	0.663	77.3	0.37	3.21	3.23	0.99
122	3.65	7.36	0.496	38.8	0.36	2.63	2.96	0.89
123	4.14	8.27	0.501	61.7	0.31	2.56	2.68	0.95
124	4.7	7.71	0.610	57.7	0.39	2.98	3.18	0.94
125	4.36	8.07	0.540	58.5	0.34	2.75	3.23	0.85
126	4.02	8.17	0.492	39.1	0.35	2.89	3.52	0.82
127	3.94	7.43	0.530	49.2	0.36	2.64	3.12	0.85
128	3.52	7.98	0.441	23.1	0.36	2.86	3.01	0.95
129	3.7	7.84	0.472	28.5	0.37	2.88	2.96	0.97
130	3.24	7.38	0.439	19.1	0.37	2.72	2.91	0.93
131	5.95	8.11	0.734	84.2	0.40	3.23	3.44	0.94
132	4.81	6.91	0.696	74.3	0.40	2.76	3.09	0.89
133	6.52	8.41	0.775	84.7	0.42	3.53	3.25	1.09
134	3.36	7.75	0.434	23.5	0.35	2.72	3.04	0.90
135	4.01	8.63	0.465	24.5	0.37	3.22	3.16	1.02
136	3.82	7.89	0.484	21.7	0.40	3.14	3.28	0.96
137	5.97	8.21	0.727	165.3	0.27	2.25	2.74	0.82
138	5.97	7.10	0.841	145.7	0.34	2.43	2.89	0.84
139	3.55	7.35	0.483	39.2	0.35	2.55	3.02	0.84
140	5.43	7.45	0.728	85.3	0.39	2.93	3.10	0.95
141	4.06	7.10	0.572	48.2	0.39	2.74	2.83	0.97
142	3.97	6.78	0.585	45.4	0.40	2.73	3.11	0.88
143	4.38	8.32	0.526	62.2	0.32	2.7	2.17	1.25
144	5.55	8.42	0.659	42.3	0.46	3.9	4.06	0.96
145	3.28	7.02	0.467	9.0	0.43	3.01	3.72	0.81
146	3.69	7.94	0.465	35.7	0.34	2.72	2.77	0.98
147	6.03	8.55	0.705	85.5	0.38	3.25	3.04	1.07
148	5.42	7.63	0.711	86.3	0.38	2.91	3.19	0.91
149	6.07	8.47	0.717	56.8	0.46	3.87	4.43	0.87
150	5.8	7.61	0.762	82.4	0.42	3.18	3.68	0.86
151	3.74	7.11	0.526	30.8	0.40	2.86	3.32	0.86
152	5.44	7.82	0.695	53.7	0.45	3.54	3.79	0.93
153	6.16	6.95	0.886	79.1	0.49	3.44	3.22	1.07
154	8.15	8.43	0.967	217.1	0.30	2.57	2.59	0.99

	Before Compression					After Compression		
	Wt	Volume	Wet Density	Est. MC	Est. OD Density	Wt (a)	Volume	Density
Sample Number	g	cm3	g/cm3	%	g/cm3	g	cm3	g/cm3
155	5.33	7.71	0.691	85.1	0.37	2.88	3.24	0.89
157	4.16	7.07	0.588	70.5	0.35	2.44	2.99	0.82
158	4.41	7.63	0.578	33.6	0.43	3.3	3.49	0.95
159	3.4	7.31	0.465	30.3	0.36	2.61	3.04	0.86
160	3.2	7.82	0.409	33.9	0.31	2.39	2.72	0.88
161	4.82	7.56	0.637	77.9	0.36	2.71	3.22	0.84
162	4.24	7.62	0.556	7.3	0.52	3.95	3.45	1.15
163	5.56	8.12	0.685	47.1	0.47	3.78	4.00	0.95
164	5.27	7.15	0.737	118.7	0.34	2.41	2.87	0.84
165	4.64	7.82	0.593	65.1	0.36	2.81	2.89	0.97
166	4.13	7.35	0.562	50.2	0.37	2.75	2.96	0.93
167	4.16	7.17	0.580	60.6	0.36	2.59	3.17	0.82
168	4.61	7.27	0.634	67.6	0.38	2.75	3.07	0.89
169	3.9	7.43	0.525	45.0	0.36	2.69	3.21	0.84
170	4.61	7.53	0.612	61.2	0.38	2.86	3.53	0.81
171	4.74	7.67	0.618	43.6	0.43	3.3	3.30	1.00
172	4.8	7.44	0.645	81.8	0.35	2.64	2.23	1.18
173	4.17	6.66	0.626	48.4	0.42	2.81	3.33	0.84
174	4.17	7.47	0.558	65.5	0.34	2.52	2.99	0.84
175	4.18	7.14	0.585	43.2	0.41	2.92	3.17	0.92
176	4.22	7.41	0.569	58.6	0.36	2.66	2.90	0.92
177	4.85	8.10	0.599	72.6	0.35	2.81	3.11	0.90
178	5.44	7.76	0.701	76.6	0.40	3.08	3.21	0.96
179	4.31	6.90	0.625	38.1	0.45	3.12	3.17	0.98
180	3.91	7.53	0.519	45.9	0.36	2.68	3.18	0.84
181	5.65	7.79	0.725	34.5	0.54	4.2	4.09	1.03
182	6.84	8.54	0.801	97.7	0.41	3.46	4.10	0.84
183	4.42	7.05	0.627	38.1	0.45	3.2	3.12	1.03
184	5.55	8.46	0.656	64.7	0.40	3.37	3.92	0.86
185	6.12	8.01	0.764	88.3	0.41	3.25	3.32	0.98
186	5.51	7.77	0.710	45.8	0.49	3.78	4.55	0.83
187	3.6	7.24	0.498	28.6	0.39	2.8	3.39	0.83
188	3.67	7.79	0.471	26.6	0.37	2.9	2.86	1.02
189	4.99	8.17	0.611	65.2	0.37	3.02	3.63	0.83
190	4.64	7.60	0.610	65.7	0.37	2.8	3.94	0.71
191	5.43	7.51	0.723	95.3	0.37	2.78	3.82	0.73
192	6.6	8.54	0.773	98.8	0.39	3.32	3.73	0.89
193	4.05	8.15	0.497	47.3	0.34	2.75	3.50	0.79
194	4.79	7.13	0.672	78.1	0.38	2.69	3.02	0.89
195	4.51	7.68	0.587	61.1	0.36	2.8	3.22	0.87
196	3.2	6.67	0.480	33.3	0.36	2.4	3.33	0.72

	Before Compression					After Compression		
	Wt	Volume	Wet Density	Est. MC	Est. OD Density	Wt (a)	Volume	Density
Sample Number	g	cm3	g/cm3	%	g/cm3	g	cm3	g/cm3
197	4.5	7.88	0.571	48.5	0.38	3.03	3.22	0.94
198	4.52	7.58	0.597	46.8	0.41	3.08	2.63	1.17
199	4.71	8.32	0.566	44.5	0.39	3.26	3.28	1.00
200	4.06	8.16	0.498	40.5	0.35	2.89	3.80	0.76
201	5.14	7.59	0.678	56.7	0.43	3.28	3.49	0.94
202	5.59	7.41	0.754	57.0	0.48	3.56	4.25	0.84
203	7.25	8.14	0.891	167.5	0.33	2.71	3.17	0.85
204	4.74	7.94	0.597	62.9	0.37	2.91	3.17	0.92
205	3.86	7.54	0.512	34.5	0.38	2.87	3.41	0.84
206	3.43	7.56	0.453	49.1	0.30	2.3	2.57	0.90
207	4.75	8.48	0.560	47.5	0.38	3.22	3.65	0.88
208	3.86	7.63	0.506	43.5	0.35	2.69	2.89	0.93
209	4.34	8.12	0.534	53.9	0.35	2.82	2.98	0.95
210	3.83	8.18	0.468	40.3	0.33	2.73	3.02	0.90
211	3.55	6.71	0.529	53.0	0.35	2.32	2.75	0.84
212	4.12	8.59	0.479	26.4	0.38	3.26	3.81	0.86
213	5.67	7.79	0.727	125.0	0.32	2.52	2.92	0.86
214	5.86	8.65	0.677	91.5	0.35	3.06	3.66	0.84
215	5.14	7.63	0.674	31.8	0.51	3.9	5.53	0.71
216	5.18	7.71	0.672	39.2	0.48	3.72	3.53	1.05
217	4	8.13	0.492	20.8	0.41	3.31	6.00	0.55
218	5.2	7.57	0.687	37.6	0.50	3.78	3.42	1.11
219	4.79	7.74	0.619	42.1	0.44	3.37	3.51	0.96
220	4.68	7.33	0.638	40.1	0.46	3.34	3.50	0.95
221	6.3	7.64	0.825	181.3	0.29	2.24	2.55	0.88
222	6.42	8.34	0.770	67.2	0.46	3.84	4.07	0.94
223	4.12	7.54	0.546	49.8	0.36	2.75	3.21	0.86
224	4.34	7.67	0.566	44.7	0.39	3	3.53	0.85
225	6.08	7.92	0.767	92.4	0.40	3.16	3.31	0.95
226	4.06	7.69	0.528	28.5	0.41	3.16	3.49	0.91
227	5.46	8.51	0.642	46.8	0.44	3.72	3.51	1.06
228	3.92	8.29	0.473	39.5	0.34	2.81	3.25	0.86
229	4.32	7.43	0.582	45.0	0.40	2.98	3.15	0.95
230	5.36	7.05	0.760	48.1	0.51	3.62	4.03	0.90
231	3.69	6.76	0.546	31.8	0.41	2.8	2.88	0.97
232	3.32	7.18	0.462	37.8	0.34	2.41	3.14	0.77
233	3.49	7.21	0.484	43.6	0.34	2.43	3.41	0.71
234	5.11	7.86	0.650	51.6	0.43	3.37	3.27	1.03
235	4.83	7.59	0.636	54.8	0.41	3.12	3.30	0.95
236	6.08	8.31	0.731	91.8	0.38	3.17	4.01	0.79
237	6.47	8.35	0.774	89.7	0.41	3.41	3.64	0.94

	Before Compression					After Compression		
	Wt	Volume	Wet Density	Est. MC	Est. OD Density	Wt (a)	Volume	Density
Sample Number	g	cm3	g/cm3	%	g/cm3	g	cm3	g/cm3
238	4.94	7.92	0.624	85.7	0.34	2.66	3.63	0.73
239	3.35	9.02	0.371	41.4	0.26	2.37	2.51	0.95
240	5	8.80	0.568	76.1	0.32	2.84	3.37	0.84
241	5.11	7.64	0.669	57.2	0.43	3.25	4.08	0.80
242	4.62	6.85	0.674	76.3	0.38	2.62	3.64	0.72
243	4.15	7.61	0.545	38.3	0.39	3	3.81	0.79
244	4.76	7.81	0.610	44.2	0.42	3.3	4.09	0.81

Table A2: Raw data for density and bending properties of the strands before and after VTC.

Panel ID	Width (mm)	Thickness (mm)	Length (mm)	Weight (g)	Density (kg/m^3)	MOE (GPa)	Panel ID	Width (mm)	Thickness (mm)	Length (mm)	Weight (g)	Density (kg/m^3)	MOE (GPa)
1	25.0	2.2	145.0	3.15	411.1	8.29	1*	24.9	1.4	135.9	3.01	633.8	9.97
2	26.0	2.0	145.8	3.33	445.3	8.38	2*	21.3	1.2	134.6	3.31	968.5	14.02
3	23.7	2.3	151.4	3.37	420.9	8.51	3*	23.6	1.2	135.4	2.55	650.0	14.19
4	25.5	2.1	146.3	3.24	414.4	8.59	4*	27.1	1.0	136.4	2.83	765.4	15.56
5	23.1	2.0	152.7	2.94	417.6	8.61	5*	24.9	1.1	135.9	2.94	797.9	16.22
6	24.4	2.0	146.1	3.06	442.0	8.64	6*	27.9	1.2	136.1	2.98	651.6	16.44
7	23.5	2.1	145.0	3.56	511.9	8.68	7*	27.9	1.0	136.4	2.3	632.1	16.90
8	23.9	2.1	145.8	3.07	419.3	8.73	8*	26.4	1.1	136.4	2.79	718.3	17.57
9	24.8	2.3	146.1	3.35	414.4	8.74	9*	28.2	1.1	136.1	3.19	786.5	17.75
10	26.7	2.1	145.3	3.3	419.3	8.77	10*	25.9	1.0	138.7	2.81	810.9	17.92
11	25.7	2.1	146.1	3.16	412.8	8.77	11*	27.2	1.2	134.9	3.01	711.8	17.96
12	24.4	2.1	145.3	3.46	481.0	8.80	12*	25.4	1.1	136.9	2.86	791.4	18.21
13	25.3	2.1	145.8	3.53	451.8	8.80	13*	22.9	1.1	137.7	2.9	854.8	18.30
14	25.7	2.1	145.8	3.26	424.1	9.04	14*	27.4	1.1	135.6	3.23	797.9	18.66
15	24.7	2.1	145.8	3.38	450.1	9.16	15*	26.3	1.0	135.1	3.09	838.5	18.89
16	25.0	2.0	152.7	4.15	547.6	9.25	16*	25.5	0.9	135.9	2.45	754.0	19.16
17	24.6	2.2	145.8	3.85	492.4	9.26	17*	26.4	1.1	134.9	3.08	827.1	19.40
18	23.0	2.0	145.8	3.12	476.1	9.45	18*	26.2	1.3	136.9	2.89	648.4	19.48
19	24.3	2.1	146.1	3.19	427.4	9.60	19*	27.9	1.1	136.9	3.71	879.1	19.68
20	25.2	2.0	145.5	3.62	489.1	9.61	20*	27.0	1.7	135.4	5.32	867.8	19.68
21	20.5	1.9	144.0	3.8	672.8	9.77	21*	25.4	1.0	137.2	2.64	796.3	20.17

Panel ID	Width (mm)	Thickness (mm)	Length (mm)	Weight (g)	Density (kg/m^3)	MOE (GPa)	Panel ID	Width (mm)	Thickness (mm)	Length (mm)	Weight (g)	Density (kg/m^3)	MOE (GPa)
22	26.2	2.1	144.8	3.96	516.8	9.90	22*	28.0	1.4	135.1	3.7	718.3	21.43
23	25.5	2.1	145.5	3.54	456.6	9.93	23*	26.9	1.1	135.1	3.3	841.8	21.73
24	24.8	1.9	145.8	3.18	476.1	10.09	24*	27.2	1.1	136.7	2.95	760.5	21.73
25	25.0	2.0	146.1	3.38	461.5	10.13	25*	26.7	1.0	135.9	2.92	775.1	22.36
26	20.7	2.0	144.0	3.78	641.9	10.62	26*	27.4	1.1	136.9	3.17	793.0	22.44
27	25.0	2.0	145.8	3.42	476.1	10.71	27*	25.5	1.0	135.4	2.91	841.8	23.58
28	21.4	2.1	145.5	2.82	440.4	11.65	28*	26.3	1.1	136.4	3.13	833.6	25.28
29	22.8	1.8	146.1	2.78	484.3	11.79	29*	26.9	0.7	137.4	2.08	864.5	26.03
30	21.0	1.9	144.0	2.98	520.0	11.99	30*	25.2	1.0	135.1	3.01	895.4	27.47

* The strands tested before the VTC process were different from the ones tested after VTC.

Table A3: Raw data for density and bending properties of the oriented strand composite with 20% and 40% by weight of VTC strands and their respective controls.

Panel ID	Specimen	Width (mm)	Thickness (mm)	Length (mm)	Weight (g)	Density (kg/m^3)	MOE (GPa)	MOR (MPa)
Control 1	A	76.9	15.4	406.4	263.27	554.9	7.60	56.89
Random orientaion	B	76.8	15.4	406.4	274.87	578.4	7.07	46.53
No VTC strands	C	76.8	15.5	406.4	268.18	562.8	6.60	45.96
	D	77.1	15.8	406.4	289.32	593.6	9.85	63.87
Control 2	A	76.8	15.0	406.4	281.67	611.1	8.09	51.14
Random orientaion	B	76.8	14.6	406.4	285.84	633.5	6.97	46.30
No VTC strands	C	76.9	14.7	406.4	276.59	609.7	6.28	50.70
	D	76.9	15.5	406.4	268.57	561.7	7.83	58.86
Control 3	A	76.8	15.2	406.4	271.4	578.7	7.03	39.65
Random orientaion	B	76.7	15.3	406.4	264.56	561.1	6.04	41.45
No VTC strands	C	76.8	16.0	406.4	289.62	589.6	7.75	42.64
	D	76.7	15.8	406.4	260.83	535.4	8.44	47.59
Control 1	A	76.6	15.7	406.4	257.48	532.3	10.27	51.43
Surface Strands oriented (20% wt)	B	76.8	15.7	406.4	269.6	556.3	11.03	69.06
No VTC strands	C	76.8	15.5	406.4	273.37	574.1	10.49	55.20
	D	76.5	15.9	406.4	267.37	547.6	10.24	51.14
Control 2	A	76.9	13.9	406.4	273.32	635.8	10.68	56.04
Surface Strands oriented (20% wt)	B	76.8	14.2	406.4	292.31	670.2	12.32	64.72
No VTC strands	C	76.9	14.9	406.4	295.25	643.6	11.61	74.01
	D	76.7	14.1	406.4	264.83	610.3	9.30	47.31
Control 3	A	76.8	15.9	406.4	280.85	574.0	12.59	51.98
Surface Strands oriented (20% wt)	B	76.7	16.2	406.4	304.54	610.5	13.33	64.38
No VTC strands	C	76.8	15.9	406.4	283.78	579.0	14.94	73.56
	D	76.6	15.2	406.4	283.13	607.2	11.95	62.97

Panel ID	Specimen	Width (mm)	Thickness (mm)	Length (mm)	Weight (g)	Density (kg/m^3)	MOE (GPa)	MOR (MPa)
Test panel 1	A	76.8	13.4	406.4	262.13	635.9	9.50	49.06
Surface Strands oriented (20% wt)	B	76.7	13.7	406.4	298.23	706.8	11.11	66.91
No VTC strands	C	76.8	13.7	406.4	296.74	701.0	10.00	74.07
	D	76.9	14.1	406.4	294.62	674.9	13.30	66.13
Test panel 2	A	76.9	15.7	406.4	280.99	578.8	14.02	68.32
Surface Strands oriented (20% wt)	B	76.7	15.8	406.4	297.79	610.9	14.78	69.00
No VTC strands	C	77.0	15.5	406.4	291.81	609.8	12.69	63.20
	D	76.9	14.6	406.4	265.73	589.8	11.97	55.53
Test panel 3	A	76.7	14.8	406.4	266.04	585.0	10.88	47.88
Surface Strands oriented (20% wt)	B	77.0	15.3	406.4	291.42	617.6	14.10	73.73
No VTC strands	C	76.8	15.0	406.4	287.86	623.4	12.87	75.36
	D	76.5	14.5	406.4	288.48	647.3	13.73	69.62
Control 1	A	76.7	14.6	406.4	298.26	664.0	12.61	61.57
Surface Strands oriented (40% wt)	B	76.7	14.9	406.4	293.64	642.4	12.72	57.29
No VTC strands	C	76.9	14.7	406.4	309.98	681.9	13.61	81.90
	D	76.5	15.2	406.4	289.91	621.9	12.21	59.26
Control 2	A	76.4	14.9	406.4	302.32	662.3	11.47	77.22
Surface Strands oriented (40% wt)	B	75.9	14.4	406.4	270.25	615.9	11.54	59.70
No VTC strands	C	76.8	15.5	406.4	298.2	623.5	12.77	72.49
	D	77.2	14.9	406.4	294.49	639.6	12.44	54.91
Control 3	A*	76.0	15.5	406.4	284.9	603.5	15.28	74.35
Surface Strands oriented (40% wt)	B*	76.0	15.4	406.4	273.7	583.5	12.92	61.57
No VTC strands	C*	76.3	15.6	406.4	270.38	566.4	12.55	58.46
	D*	76.3	15.4	406.4	284.61	603.6	14.45	74.63
Test panel 1	A	77.0	15.0	406.4	298.92	645.4	17.67	89.95
Surface Strands oriented (40% wt)	B	76.8	14.8	406.4	300.51	657.4	17.75	87.36
No VTC strands	C	77.0	14.8	406.4	299.04	656.2	16.38	78.97
	D	76.8	14.9	406.4	284.93	619.0	13.90	70.68
Test panel 2	A	76.8	13.3	406.4	303.43	738.8	13.20	73.00
Surface Strands oriented (40% wt)	B	76.6	13.9	406.4	289.36	677.1	13.30	67.38
No VTC strands	C	76.9	13.7	406.4	302.45	713.6	13.42	66.70
	D	77.1	13.6	406.4	312.87	744.9	13.49	70.47

Panel ID	Specimen	Width (mm)	Thickness (mm)	Length (mm)	Weight (g)	Density (kg/m^3)	MOE (GPa)	MOR (MPa)
Test panel 3	A	76.8	15.7	406.4	294.36	608.7	17.10	83.59
Surface Strands oriented (40% wt)	B	76.7	16.0	406.4	313.3	637.9	19.00	80.55
No VTC strands	C	76.8	15.9	406.4	319.85	651.3	19.52	77.96
	D	76.6	15.7	406.4	314.53	653.7	18.44	78.81

*Data not included in the statistical analysis due to inconsistency in processing procedures.

Table A4: Thickness swell of the oriented strand composite with 20% and 40% by weight of VTC strands and their respective controls.

		Initial Dimensions							Thickness Swell (%)		
		Thickness (mm)				Width	Length				
Panel ID	Specimen	Location1	Location2	Location3	Location4	(inches)	(inches)	Weight (g)	2-hr	24-hr	Redry
Control 1 Random orientaion (No VTC strands)	A	15.49	15.4	15	15.23	6.0085	6.009	212.88	0.0782	0.2057	0.1698
	B	15.55	15.79	15.49	15.29	6.0085	6.01	205.81	0.0707	0.2003	0.1665
Control 2 Random orientaion (No VTC strands)	A	14.51	14.9	14.51	14.36	6.006	6.004	175.94	0.0659	0.1568	0.0863
	B	15.33	15.29	15.22	15.19	6.013	6.0105	203.13	0.0626	0.1960	0.1527
Control 3 Random orientaion (No VTC strands)	A	15.86	15.83	15.51	15.77	6.0035	6.006	194.91	0.0797	0.2003	0.1504
	B	16.25	15.93	15.86	15.48	6.0085	6.0095	208.62	0.0809	0.2127	0.1644
Control 1 Surface Strands oriented (20% wt) (No VTC strands)	A	16.31	15.41	15.6	15.83	6.0145	6.006	232.66	0.0584	0.1905	0.1848
	B	15.72	15.47	15.81	16.06	6.0105	5.995	211.28	0.0898	0.2325	0.1954
Control 2 Surface Strands oriented (20% wt) (No VTC strands)	A	13.91	13.71	14.05	13.97	6.002	6.0105	196.03	0.0537	0.1758	0.1476
	B	15.09	14.43	14.17	14.13	6.016	6.008	208.24	0.0470	0.1354	0.1067
Control 3 Surface Strands oriented (20% wt) (No VTC strands)	A	15.63	15.75	15.96	15.46	6.0115	5.97	221.09	0.0694	0.2021	0.1941
	B	15.82	15.73	15.39	15.4	6.016	6.004	206.44	0.0892	0.1877	0.1412
Test Panel 1 Surface Strands oriented (20% wt VTC strands)	A	13.88	13.92	13.84	13.99	6.014	6.008	211.72	0.1406	0.3115	0.3076
	B	14.81	14.49	14.18	14.43	6.013	6.0035	236.34	0.0466	0.2096	0.1601
Test Panel 2 Surface Strands oriented (20% wt VTC strands)	A	15.29	14.97	15.39	15.25	6.019	6.001	221.32	0.0882	0.2255	0.1898
	B	15.44	14.74	15.29	15.39	6.011	6.014	214.63	0.0905	0.1903	0.1267
Test Panel 3 Surface Strands oriented (20% wt VTC strands)	A	14.92	14.95	15.06	15.07	6.0095	5.9815	198.65	0.1572	0.2397	0.1497
	B	14.47	14.57	14.97	15.03	6.015	6.007	210.91	0.0967	0.2304	0.1682

		Initial Dimensions							Thickness Swell (%)		
		Thickness (mm)				Width (inches)	Length (inches)	Weight (g)	2-hr	24-hr	Redry
Panel ID	Specimen	Location1	Location2	Location3	Location4						
Control 1 Random orientaion (No VTC strands)	A	15.49	15.4	15	15.23	6.0085	6.009	212.88	0.0782	0.2057	0.1698
Control 1 Surface Strands oriented (40% wt) (No VTC strands)	A	14.79	14.97	14.79	14.68	6.018	6.002	221.63	0.0287	0.1413	0.1362
	B	14.88	14.87	14.76	14.62	6.019	6.007	201.51	0.0446	0.1671	0.1397
Control 2 Surface Strands oriented (40% wt) (No VTC strands)	A	14.1	14.59	13.93	13.68	6.0195	6.02	197.11	0.0561	0.1751	0.1407
	B	14.44	14.76	15.69	14.96	6.019	6.0065	210.52	0.0424	0.1315	0.0887
Control 3 Surface Strands oriented (40% wt) (No VTC strands)	A*	15.36	15.36	15.41	15.52	5.9675	5.9565	208.1	0.1296	0.3011	0.2725
	B*	15.22	15.61	15.04	15.47	5.966	5.962	199.68	0.1422	0.2936	0.2788
Test Panel 1 Surface Strands oriented (40% wt VTC strands)	A	14.76	14.62	14.95	14.99	6.0155	6	216.25	0.1032	0.2385	0.1907
	B	14.36	15.66	14.68	15.02	6.004	6.0135	224.19	0.1011	0.2324	0.1551
Test Panel 2 Surface Strands oriented (40% wt VTC strands)	A	13.98	13.87	13.97	13.73	6.0225	6.0045	220.17	0.0733	0.2383	0.2023
	B	13.4	13.44	13.44	13.77	6.026	6.009	212.46	0.1378	0.2422	0.1667
Test Panel 3 Surface Strands oriented (40% wt VTC strands)	A	15.89	15.77	15.53	15.59	6.0195	6.0045	225.69	0.1115	0.2354	0.1526
	B	15.68	16.19	15.49	15.68	6.0125	6.0075	223.95	0.1315	0.2514	0.1759

*Data included in the statistical analysis due to inconsistency in processing procedures.

Table A5: Raw density data and internal bond data of the oriented strand composite with 20% and 40% by weight of VTC strands and their respective controls.

		Length (mm)	Width (mm)	Thickness (mm)	Weight (gm)	Density (gm/cm3)	IB (KPa)
1	C1ROA	50.96	51.41	15.88	21.14	0.51	675.5
2	C1ROB	50.92	52.04	15.64	21.33	0.51	682.4
3	C1ROC	51.43	50.94	15.65	25.45	0.62	850.6
4	C1ROD	51.44	51.62	15.56	23.33	0.56	754.1
5	C1ROE	51.23	51.03	15.66	24.15	0.59	838.2
6	C1ROF	51.31	51.33	15.56	26.39	0.64	624.5
7	C1ROG	51.56	51.37	16.3	30.59	0.71	736.1
8	C1ROH	51.78	51.17	15.5	22.39	0.55	532.8
9	C1ROI	51.2	51.75	15.49	23.59	0.57	667.2
10	C2ROA	51.6	50.97	15.5	0.00	0.00	554.9
11	C2ROB	50.88	52.26	15.56	21.96	0.53	695.5
12	C2ROC	51.56	50.98	15.41	25.78	0.64	777.5
13	C2ROD	51.37	51.64	15.45	25.08	0.61	652.0
14	C2ROE	51.35	51.75	15.49	24.03	0.58	795.4
15	C2ROF	51.35	51.65	15.32	24.32	0.60	953.9
16	C2ROG	51.37	51.49	15.24	26.31	0.65	890.5
17	C2ROH	51.34	51.33	15.4	26.02	0.64	973.2
18	C2ROI	51.32	51.47	15.11	21.7	0.54	946.4
19	C3ROA	51.01	51.63	16.07	21.13	0.50	831.9
20	C3ROB	50.89	51.86	15.94	20.08	0.48	645.8
21	C3ROC	50.94	51.51	15.84	20.96	0.50	662.4
22	C3ROD	51.89	51.36	15.86	23.18	0.55	497.0
23	C3ROE	51.45	51.25	15.82	21.17	0.51	807.1
24	C3ROF	51.36	51.36	15.82	22.34	0.54	776.8
25	C3ROG	51.38	51.42	15.94	24.58	0.58	736.1
26	C3ROH	52.17	51	15.94	21.25	0.50	596.9
27	C3ROI	51.11	51.29	16.23	23.34	0.55	602.4
28	C1O2A	51.48	50.92	15.84	25.21	0.61	814.0
29	C1O2B	50.93	51.47	15.94	23.06	0.55	882.3
30	C1O2C	50.91	51.66	15.78	21.31	0.51	765.8
31	C1O2D	51.35	51.84	15.93	25.89	0.61	724.4
32	C1O2E	51.26	51.05	15.86	26.5	0.64	956.0
33	C1O2F	51.3	51.65	15.47	22.5	0.55	696.2
34	C1O2G	51.22	52.04	15.69	24.89	0.60	634.1
35	C1O2H	51.24	51.21	16.04	26.48	0.63	727.9
36	C1O2I	51.31	51.07	15.57	21.2	0.52	822.3
37	C2O2A	50.95	51.7	15.07	27.16	0.68	647.2

		Length (mm)	Width (mm)	Thickness (mm)	Weight (gm)	Density (gm/cm3)	IB (KPa)
38	C2O2B	51.75	50.88	14.5	23.61	0.62	981.5
39	C2O2C	51.41	50.98	14.25	22.9	0.61	610.7
40	C2O2D	51.41	51.61	14.63	23.43	0.60	814.0
41	C2O2E	51.3	51.78	14.68	25.27	0.65	896.1
42	C2O2F	51.37	51.55	14.47	23.6	0.62	783.7
43	C2O2G	51.32	51.89	14.24	19.35	0.51	886.4
44	C2O2H	51.41	51.41	14.31	25.21	0.67	1018.7
45	C2O2I	51.27	51.47	14.44	22.91	0.60	719.6
46	C3O2A	51	51.31	15.94	24.67	0.59	605.2
47	C3O2B	50.87	51.81	15.79	22.85	0.55	824.4
48	C3O2C	51.26	50.88	15.74	21.26	0.52	621.0
49	C3O2D	51.09	51.34	15.69	25.12	0.61	554.2
50	C3O2E	51.81	51.14	15.7	24.45	0.59	652.7
51	C3O2F	51.49	51.32	15.69	22.77	0.55	723.0
52	C3O2G	51.61	51.31	15.87	24.63	0.59	779.6
53	C3O2H	51.34	51.09	15.34	23.81	0.59	687.9
54	C3O2I	51.16	51.25	15.29	19.95	0.50	800.9
55	T1O2A	50.95	51.25	14.41	22.89	0.61	652.7
56	T1O2B	50.89	52.05	14.98	25.53	0.64	773.4
57	T1O2C	50.97	51.27	14.53	25.5	0.67	935.3
58	T1O2D	51.96	51.35	13.85	24.44	0.66	900.2
59	T1O2E	51.43	51.38	13.85	22.22	0.61	746.5
60	T1O2F	51.56	51.23	13.88	21.75	0.59	847.1
61	T1O2G	51.38	51.45	14.01	25.68	0.69	821.6
62	T1O2H	51.41	51.55	13.9	23.42	0.64	566.6
63	T1O2I	51.42	51.9	14	23.17	0.62	690.0
64	T2O2A	51	51.21	15.49	24.1	0.60	816.1
65	T2O2B	50.89	52.03	15.28	20.26	0.50	649.3
66	T2O2C	50.97	51.68	15.22	23.58	0.59	825.1
67	T2O2D	51.4	51.18	15.15	24.74	0.62	803.7
68	T2O2E	51.2	52.35	15.04	21.59	0.54	680.3
69	T2O2F	51.38	51.41	15.09	22.95	0.58	783.0
70	T2O2G	51.4	51.49	15.18	22.49	0.56	744.4
71	T2O2H	51.27	51.67	14.97	19.35	0.49	555.6
72	T2O2I	51.35	51.01	15.01	20.78	0.53	803.7
73	T3O2A	51.56	50.95	15.4	26.43	0.65	492.1
74	T3O2B	50.97	51.42	15.6	27.17	0.66	530.7
75	T3O2C	51	51.25	15.07	25.47	0.65	758.9
76	T3O2D	51.37	52.16	14.82	31.44	0.79	810.6
77	T3O2E	51.33	51.45	15.17	28.33	0.71	809.2
78	T3O2F	51.38	50.86	14.79	22.59	0.58	721.7
79	T3O2G	51.34	51.51	15.14	27.65	0.69	862.3
80	T3O2H	51.45	51.31	14.69	24.92	0.64	496.3
81	T3O2I	51.07	51.24	14.86	25	0.64	670.7
82	C1O4A	50.94	51.3	15	26.39	0.67	906.4
83	C1O4B	51.86	50.95	14.84	22.87	0.58	1002.9
84	C1O4C	51.42	50.91	14.84	25.42	0.65	997.4

		Length (mm)	Width (mm)	Thickness (mm)	Weight (gm)	Density (gm/cm3)	IB (kPa)
85	C1O4D	51.36	51.46	15.13	24.43	0.61	965.0
86	C1O4E	51.24	51.87	15.05	24.19	0.60	986.3
87	C1O4F	51.68	51.36	14.95	27.84	0.70	931.2
88	C1O4G	51.33	51.06	15.12	22.12	0.56	559.0
89	C1O4H	52.16	51.33	15.09	24.09	0.60	542.5
90	C1O4I	51.05	51.47	15.35	24.53	0.61	792.7
91	C2O4A	50.93	51.22	16.62	24.46	0.56	646.5
92	C2O4B	51.65	50.93	15.14	26	0.65	737.5
93	C2O4C	51.26	50.95	15.67	24.08	0.59	911.9
94	C2O4D	51.34	51.65	16.01	26.39	0.62	885.0
95	C2O4E	51.6	51.35	15.23	25.76	0.64	887.8
96	C2O4F	51.41	51.76	15.03	24.66	0.62	727.9
97	C2O4G	51.37	51.73	14.47	23.82	0.62	1067.7
98	C2O4H	51.28	51.51	14.51	24.07	0.63	985.0
99	C2O4I	51.27	51.35	14.4	23.52	0.62	696.9
100*	C3O4A	50.67	51.88	15.66	25.32	0.62	909.8
101*	C3O4B	51.45	50.72	15.48	23.84	0.59	667.9
102*	C3O4C	51.47	50.73	15.53	21.79	0.54	840.2
103*	C3O4D	50.55	51.85	15.35	20.35	0.51	472.1
104*	C3O4E	52.02	50.58	15.43	22.46	0.55	561.8
105*	C3O4F	51.21	50.48	15.38	23.51	0.59	867.1
106*	C3O4G	51.81	50.53	15.47	23.02	0.57	811.3
107*	C3O4H	51.69	50.61	15.23	24.42	0.61	832.6
108*	C3O4I	51.36	50.53	15.15	23.82	0.61	742.3
109	T1O4A	51.34	50.95	15.15	25.51	0.64	739.6
110	T1O4B	50.85	51.9	14.88	25.06	0.64	633.4
111	T1O4C	51.01	51.57	14.78	25.6	0.66	677.6
112	T1O4D	51.28	51.63	14.63	27.47	0.71	787.1
113	T1O4E	51.71	51.23	14.61	24.9	0.64	264.0
114	T1O4F	51.36	51.33	15.1	25.62	0.64	697.5
115	T1O4G	51.41	51.26	14.91	25.39	0.65	452.2
116	T1O4H	51.38	52	14.51	24.8	0.64	616.2
117	T1O4I	51.41	51.33	14.86	26.18	0.67	673.4
118	T2O4A	50.9	51.95	14.01	22.76	0.61	805.8
119	T2O4B	50.8	51.03	15.19	27.55	0.70	905.0
120	T2O4C	51.54	50.97	13.92	24.49	0.67	1065.6
121	T2O4D	51.37	51.46	13.77	25.05	0.69	995.3
122	T2O4E	51.24	51.67	13.75	24.72	0.68	951.9
123	T2O4F	51.33	51.72	13.63	25.21	0.70	773.4
124	T2O4G	51.37	51.98	13.63	26.33	0.72	949.8
125	T2O4H	51.53	51.31	13.25	25.23	0.72	1089.0
126	T2O4I	51.13	51.26	13.59	22.8	0.64	1049.8
127	T3O4A	50.86	51.87	16.34	22.77	0.53	581.1
128	T3O4B	50.84	51.56	15.96	23.89	0.57	396.3
129	T3O4C	50.9	51.41	15.43	21.41	0.53	569.3
130	T3O4D	51.26	51.73	15.91	28.35	0.67	894.7
131	T3O4E	51.43	51.32	16.44	30.9	0.71	840.9

		Length (mm)	Width (mm)	Thickness (mm)	Weight (gm)	Density (gm/cm3)	IB (kPa)
132	T3O4F	50.7	51.37	16.84	27.74	0.63	790.6
133	T3O4G	51.37	51.53	15.94	27.65	0.66	809.9
134	T3O4H	51.27	51.69	15.65	26.59	0.64	1016.0
135	T3O4I	51.3	51.55	15.94	30.76	0.73	670.7

*Data not included in the statistical analysis due to inconsistency in processing procedures.

Appendix B: Raw data for strand composite modified by the VTC process.

Table B1: Raw data for density and MOE of the 16-inch by 9-inch by ¼-inch strand board, before VTC processing.

Before VTC							
Spacer thickness (mm)	**Panel Code**	**Weight (gm)**	**Width (cm)**	**Thickness (mm)**	**Length (cm)**	**Density (kg/m^3)**	**MOE (GPa)**
0	P5E	392.19	24.97	7.91	40.64	492.4	3.86
0	P5B	415.21	24.94	7.88	40.64	523.4	3.69
0	P3B	423.36	24.94	9.33	40.64	450.8	2.22
0	P5C	430.48	24.97	7.82	40.64	546.5	3.51
0.42	P2F	478.11	24.89	7.26	40.64	655.7	4.77
0.42	P8F	432.53	24.89	7.76	40.64	554.9	3.79
0.42	P6C	437.00	24.89	8.94	40.64	486.7	3.52
0.42	P5F	451.81	24.89	8.33	40.64	540.0	3.40
0.86	P1E	467.55	24.97	8.71	40.64	533.2	3.47
0.86	P1B	407.98	24.97	8.66	40.64	467.8	3.16
0.86	P6E	445.36	24.97	9.07	40.64	487.5	3.21
0.86	P7F	433.40	24.89	8.40	40.64	513.7	4.12

* Initial dimensions are based on nominal 12% MC at 20^{o}C and 65% RH.

Table B2: Raw data for density and MOE of the strand board, after VTC processing.

After VTC							
Spacer thickness (mm)	**Panel Code**	**Weight (gm)**	**Width (cm)**	**Thickness (mm)**	**Length (cm)**	**Density (kg/m^3)**	**MOE (GPa)**
0	P5E	423.14	24.94	3.98	40.64	1056.4	9.82
0	P5B	408.21	24.94	3.50	40.64	1159.0	9.62
0	P3B	420.46	24.94	4.39	40.64	951.8	5.46
0	P5C	424.30	24.94	4.03	40.64	1046.2	9.25
0.42	P2F	469.57	24.94	4.20	40.64	1111.0	9.47
0.42	P8F	423.26	24.94	3.84	40.64	1095.3	10.24
0.42	P6C	427.70	24.94	3.99	40.64	1065.2	10.40
0.42	P5F	441.18	24.94	3.99	40.64	1098.7	10.55
0.86	P1E	463.68	24.94	4.52	40.64	1019.4	8.34
0.86	P1B	430.46	24.94	4.41	40.64	970.0	7.51
0.86	P6E	440.62	24.94	4.40	40.64	995.0	8.45
0.86	P7F	425.53	24.94	4.04	40.64	1046.7	10.88

Table B3: Raw data for density and bending properties of the three layered laminate composite.

	Panel Code	Target Degree of Densification (%)	Weight (gm)	Width (cm)	Thickness (cm)	Length (cm)	Density (Kg/m^3)	MOE (GPa)	MOR (MPa)
1	P1BA	71	400.13	7.62	1.75	40.64	749.9	5.74	33.77
2	P1BB		418.19	7.62	1.80	40.64	758.9	6.65	39.98
3	P1BC		432.20	7.62	1.73	40.64	819.0	6.88	46.18
4	P8FA	94	408.87	7.62	1.63	40.64	823.2	5.92	43.42
5	P8FB		415.40	7.62	1.78	40.64	764.7	6.28	43.42
6	P8FC		405.68	7.62	1.71	40.64	777.2	5.71	31.02
7	P6CA		426.00	7.62	1.75	40.64	795.6	7.08	46.18
8	P6CB		405.70	7.62	1.83	40.64	726.1	6.98	50.32
9	P6CC		404.26	7.62	1.73	40.64	763.3	6.25	40.67
10	P5CA	122	389.84	7.62	1.65	40.64	772.9	5.75	37.91
11	P5CB		396.26	7.62	1.71	40.64	756.4	5.92	34.46
12	P5CC		424.26	7.62	1.74	40.64	796.9	6.39	35.84
13	P5EA		424.67	7.62	1.96	40.64	710.6	5.76	36.53
14	P5EB		403.18	7.62	1.89	40.64	697.3	5.38	33.08
15	P5EC		404.94	7.62	1.78	40.64	745.4	4.40	28.56

B4: Theoretical Sample Computation for the MOE of the three layered composite.

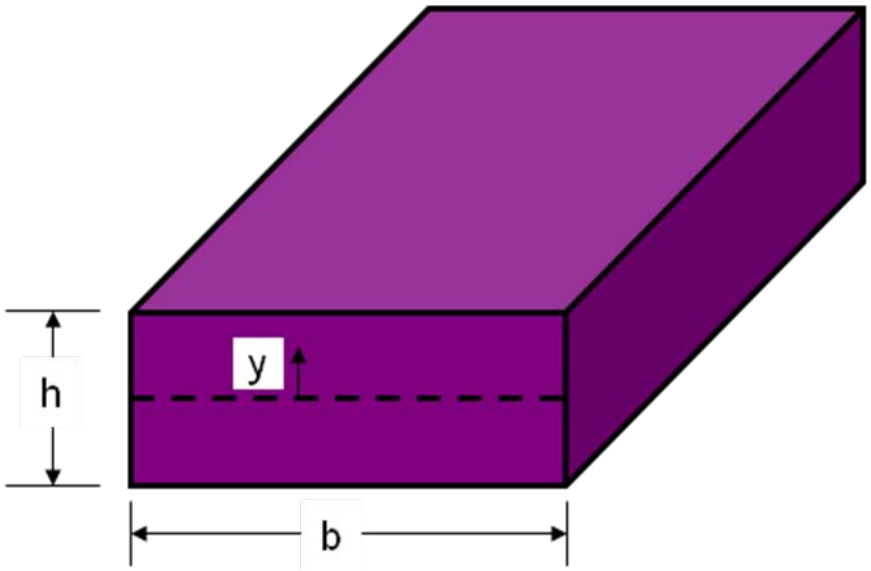

Moment of Inertia of a rectangular section = $$I = \int_{-h/2}^{h/2} by^2 dy = \frac{bh^3}{12}$$

For the three layered composite, the integration for the moment of inertia was done in parts and I' was computed to be:

$$I' = \frac{1}{12}\left[b_c d_c^3 + b_f d^3 - b_f d_c^3\right]$$

Where, b = width of layer, d = thickness of layer, E = bending modulus of layer, c = subscript for core layer, f = subscript for face layer

Assuming that the contribution of each layer to bending stiffness is proportional to the width of each layer, then:

$$\frac{b_c}{b_f} = \frac{E_c}{E_f}$$

The effective modulus is then: $E' = (E_f I')/I$

Sample Calculation:

$E_f = 1578$ ksi

$E_c = 594$ ksi

$b_c = b_f = 3$ inch

$d_c = 0.34$ inch

$d_f = 0.16$ inch

Substitiution of the above values in the formulae given below yields:

Effective Modulus = 1232 ksi.

Appendix C: Statistical results obtained using S-PLUS.

Result C1: Statistical summary of the MOE data of the oriented strand composite with 20% and 40% by weight of VTC strands and their respective controls.

```
*** Analysis of Variance Model ***

Short Output:
Call:
   aov(formula = C2 ~ C1, data = MOE.ANOVA.data, na.action = na.exclude)

Terms:
                      C1 Residuals
 Sum of Squares 9735710   2545562
Deg. of Freedom       4        47

Residual standard error: 232.7249
Estimated effects may be unbalanced

          Df Sum of Sq Mean Sq  F Value         Pr(F)
       C1  4   9735710 2433928 44.93884 1.665335e-015
Residuals 47   2545562   54161


95 % simultaneous confidence intervals for specified
linear combinations, by the Tukey method

critical point: 2.8365
response variable: C2

intervals excluding 0 are flagged by '****'

    Estimate Std.Error Lower Bound Upper Bound
A-B     -595        95        -865      -326.0 ****
A-C     -822       106       -1120      -521.0 ****
A-D     -719       106       -1020      -418.0 ****
A-E    -1250        95       -1520      -983.0 ****
B-C     -227       106        -529        73.9
B-D     -124       106        -425       177.0
B-E     -658        95        -927      -388.0 ****
C-D      103       116        -227       433.0
C-E     -431       106        -732      -129.0 ****
D-E     -534       106        -835      -232.0 ****
```

**** indicates that there is statistically significant difference between the treatments.

Result C2: Statistical summary of the MOR data of the oriented strand composite with 20% and 40% by weight of VTC strands and their respective controls.

```
*** Analysis of Variance Model ***

Short Output:
Call:
   aov(formula = C2 ~ C1, data = MOR.ANOVA.data, na.action = na.exclude)

Terms:
                       C1 Residuals
 Sum of Squares 101752636  80880642
Deg. of Freedom         4        51

Residual standard error: 1259.323
Estimated effects may be unbalanced

          Df Sum of Sq  Mean Sq  F Value        Pr(F)
       C1  4 101752636 25438159 16.04025 1.45143e-008
Residuals 51  80880642  1585895


95 % simultaneous confidence intervals for specified
linear combinations, by the Tukey method

critical point: 2.8278
response variable: C2

intervals excluding 0 are flagged by '****'

    Estimate Std.Error Lower Bound Upper Bound
A-B    -1570       514       -3030      -121.0 ****
A-C    -2260       514       -3720      -810.0 ****
A-D    -2360       575       -3980      -731.0 ****
A-E    -4040       514       -5490     -2580.0 ****
B-C     -689       514       -2140       765.0
B-D     -782       575       -2410       843.0
B-E    -2460       514       -3920     -1010.0 ****
C-D      -93       575       -1720      1530.0
C-E    -1770       514       -3230      -319.0 ****
D-E    -1680       575       -3310       -54.3 ****
```

**** indicates that there is statistically significant difference between the treatments.

Result C3: Statistical summary of the IB data of the oriented strand composite with 20% and 40% by weight of VTC strands and their respective controls.

```
*** Analysis of Variance Model ***


Short Output:
Call:
   aov(formula = C2 ~ C1, data = IB.ANOVA.data, na.action = na.exclude)

Terms:
                      C1 Residuals
 Sum of Squares  3745.38  58239.03
Deg. of Freedom        4       121

Residual standard error: 21.93888
Estimated effects may be unbalanced

           Df Sum of Sq  Mean Sq  F Value     Pr(F)
       C1   4   3745.38 936.3456 1.945393 0.1072379
Residuals 121  58239.03 481.3143


95 % simultaneous confidence intervals for specified
linear combinations, by the Tukey method

critical point: 2.7693
response variable: C2

intervals excluding 0 are flagged by '****'

    Estimate Std.Error Lower Bound Upper Bound
A-B  -4.6900      5.97      -21.20       11.80
A-C   0.0556      5.97      -16.50       16.60
A-D -16.6000      6.68      -35.10        1.90
A-E  -5.0400      5.97      -21.60       11.50
B-C   4.7400      5.97      -11.80       21.30
B-D -11.9000      6.68      -30.40        6.59
B-E  -0.3560      5.97      -16.90       16.20
C-D -16.6000      6.68      -35.10        1.84
C-E  -5.1000      5.97      -21.60       11.40
D-E  11.5000      6.68       -6.94       30.00
```

Result C4: Statistical summary of the TS – 2hr data of the oriented strand composite with 20% and 40% by weight of VTC strands and their respective controls.

```
*** Analysis of Variance Model ***

Short Output:
Call:
   aov(formula = X2.hr ~ Col1, data = TS.ANOVA.data, na.action = na.exclude)

Terms:
                      Col1  Residuals
 Sum of Squares 0.01510159 0.01298902
Deg. of Freedom          4         23

Residual standard error: 0.02376426
Estimated effects may be unbalanced

          Df  Sum of Sq     Mean Sq  F Value       Pr(F)
     Col1  4 0.01510159 0.003775397 6.685195 0.001009129
Residuals 23 0.01298902 0.000564740


95 % simultaneous confidence intervals for specified
linear combinations, by the Tukey method

critical point: 2.956
response variable: X2.hr

intervals excluding 0 are flagged by '****'

    Estimate Std.Error Lower Bound Upper Bound
A-B  0.00507    0.0137     -0.0355     0.04560
A-C -0.03030    0.0137     -0.0709     0.01030
A-D  0.03000    0.0153     -0.0153     0.07540
A-E -0.03670    0.0137     -0.0773     0.00382
B-C -0.03540    0.0137     -0.0759     0.00519
B-D  0.02500    0.0153     -0.0204     0.07030
B-E -0.04180    0.0137     -0.0824    -0.00125 ****
C-D  0.06030    0.0153      0.0150     0.10600 ****
C-E -0.00644    0.0137     -0.0470     0.03410
D-E -0.06680    0.0153     -0.1120    -0.02140 ****
```

**** indicates that there is statistically significant difference between the treatments.

Result C5: Statistical summary of the TS – 24hr data of the oriented strand composite with 20% and 40% by weight of VTC strands and their respective controls.

```
*** Analysis of Variance Model ***

Short Output:
Call:
   aov(formula = X24.hr ~ Col1, data = TS.ANOVA.data, na.action = na.exclude)

Terms:
                      Col1  Residuals
 Sum of Squares 0.02538640 0.01716901
Deg. of Freedom          4         23

Residual standard error: 0.02732177
Estimated effects may be unbalanced

          Df  Sum of Sq     Mean Sq  F Value       Pr(F)
     Col1  4 0.02538640 0.006346599 8.502047 0.000230161
Residuals 23 0.01716901 0.000746479


95 % simultaneous confidence intervals for specified
linear combinations, by the Tukey method

critical point: 2.956
response variable: X24.hr

intervals excluding 0 are flagged by '****'

    Estimate Std.Error Lower Bound Upper Bound
A-B  0.00796    0.0158     -0.0387    0.054600
A-C -0.03920    0.0158     -0.0858    0.007420
A-D  0.04150    0.0176     -0.0106    0.093700
A-E -0.04440    0.0158     -0.0911    0.002180
B-C -0.04720    0.0158     -0.0938   -0.000535 ****
B-D  0.03360    0.0176     -0.0186    0.085700
B-E -0.05240    0.0158     -0.0990   -0.005770 ****
C-D  0.08070    0.0176      0.0286    0.133000 ****
C-E -0.00524    0.0158     -0.0519    0.041400
D-E -0.08600    0.0176     -0.1380   -0.033800 ****
```

**** indicates that there is statistically significant difference between the treatments.

Result C6: Statistical summary of the TS – Redried data of the oriented strand composite with 20% and 40% by weight of VTC strands and their respective controls.

```
*** Analysis of Variance Model ***

Short Output:
Call:
   aov(formula = Redry ~ Col1, data = TS.ANOVA.data, na.action = na.exclude)

Terms:
                      Col1  Residuals
 Sum of Squares 0.00984842 0.03572102
Deg. of Freedom          4         23

Residual standard error: 0.03940923
Estimated effects may be unbalanced

           Df  Sum of Sq     Mean Sq  F Value     Pr(F)
     Col1   4 0.00984842 0.002462105 1.585297 0.2118973
Residuals 23 0.03572102 0.001553088


95 % simultaneous confidence intervals for specified
linear combinations, by the Tukey method

critical point: 2.956
response variable: Redry

intervals excluding 0 are flagged by '****'

    Estimate Std.Error Lower Bound Upper Bound
A-B -0.01330    0.0228     -0.0805      0.0540
A-C -0.03530    0.0228     -0.1030      0.0319
A-D  0.02200    0.0254     -0.0532      0.0972
A-E -0.02550    0.0228     -0.0928      0.0417
B-C -0.02210    0.0228     -0.0893      0.0452
B-D  0.03530    0.0254     -0.0399      0.1100
B-E -0.01230    0.0228     -0.0795      0.0550
C-D  0.05730    0.0254     -0.0179      0.1330
C-E  0.00979    0.0228     -0.0575      0.0770
D-E -0.04750    0.0254     -0.1230      0.0277
```